Available online at www.sciencedirect.com
SCIENCE DIRECT®
Computers and Structures 83 (2005) 934–955
Computers & Structures
www.elsevier.com/locate/compstruc

Vibrations of thick isotropic plates with higher order shear and normal deformable Plate theories

R.C. Batra *, S. Aimmanee

Department of Engineering Science and Mechanics, MC 0219 Virginia Polytechnic Institute and State University Blacksburg, VA 24061, United States

Received 19 February 2004; accepted 11 November 2004

R.C. Batra dedicates this work to Professor J.N. Reddy on his 60th birthday

Abstract

We use a higher order shear and normal deformable plate theory of Batra and Vidoli and the finite element method to analyze free vibrations and stress distribution in a thick isotropic and homogeneous plate. The transverse shear and the transverse normal stresses and strains in the plate are considered and traction boundary conditions on the top and the bottom surfaces of the plate are exactly satisfied. All components of the stress tensor are computed from equations of the plate theory. Equations governing deformations of the plate involve second-order spatial derivatives of generalized displacements with respect to in-plane coordinates. Thus triangular or quadrilateral elements with Lagrange basis functions can be employed to find their numerical solution. Results have been computed for rectangular plates of aspect ratios varying from 4 to 20 and with all edges either simply supported or clamped, or two opposite edges clamped and the other two free. Computed frequencies, mode shapes, and through the thickness distribution of stresses for a simply supported plate are found to match very well with the corresponding analytical solutions. Advantages of the present approach include the use of Lagrange shape functions, satisfaction of traction boundary conditions on the top and the bottom surfaces and the use of the plate theory equations for accurate determination of transverse stresses. The order of the plate theory to be used depends upon several factors including the aspect ratio of the plate.

Keywords: Rectangular plate; Natural frequencies; Stress distribution; Finite element method; Simply supported; Clamped and free edges

1. Introduction

Whereas many higher-order plate theories (e.g. see [1,2]) neglect transverse normal strains, those derived by Mindlin and Medick [3], Soldatos and Watson [4], Babu and Kant [5], Chao et al. [6], Lee and Yu [7], Batra and Vidoli [8], Messina [9], Carrera [10], DiCarlo et al. [11] and the Cosserat brothers [12], amongst others, consider them. Transverse normal deformations are significant in thick plates and also in laminated plates with laminae having widely different elastic constants. Exceptions to the usual expansions of the mechanical displacements as a power series in the thickness coordinate are,

* Corresponding author. Tel.: +1 540 231 6051; fax: +1 540 231 4574.
E-mail address: rbatra@vt.edu (R.C. Batra).

0045-7949/$ - see front matter © 2005 Elsevier Ltd. All rights reserved.
doi:10.1016/j.compstruc.2004.11.023

amongst others, works of Soldatos and Watson [4], Mindlin and Medick [3], Lee and Yu [7], and Batra and Vidoli [8] who respectively use exponential functions, Legendre polynomials, trignometric functions and Legendre polynomials. Higher-order plate theories derived by using different basis functions are not necessarily equivalent since the first-order theory of Lee and Yu [7] involves $\cos(\pi(1-z)/2)$, where z $(-1 \leqslant z \leqslant 1)$ is the normalized thickness coordinate, and the first-order theory of Mindlin and Medick [3] expresses mechanical displacements as an affine function of z. A plate theory is usually called higher order if terms up to and including z^K with $K \geqslant 3$ are retained in the expansions for displacements. The optimal value of K so that results from the plate theory match with the exact solution of the 3-dimensional elasticity equations depends upon the aspect ratio of the plate, boundary conditions prescribed at the edges, material symmetries, material inhomogeneities, applied loads and which aspects of the three-dimensional deformations should be accurately modeled. Batra and Vidoli's [8] Kth-order plate theory differs from earlier (e.g. [3,7]) higher-order plate theories at least in the following respects. Batra and Vidoli [8] express the transverse shear stresses and the transverse normal stress as polynomials of degree $K+2$ in z, with the remaining variables expanded as polynomials of degree K in z. The normal and the tangential surface tractions prescribed on the top and the bottom surfaces of the plate appear explicitly in the two-dimensional constitutive relations thereby exactly satisfying natural boundary conditions prescribed on these surfaces. The transverse shear and the transverse normal stresses are computed from the plate equations rather than by integrating a posteriori the three-dimensional equations of elasticity.

Batra et al. [13] studied vibrations of, and the propagation of plane waves in, thick simply supported rectangular orthotropic plates with the Kth-order plate theory of Batra and Vidoli [8]. Following Srinivas et al. [14] they expanded different components of the generalized displacements of the plate theory in terms of trignometric functions defined on the midsurface of the plate. The assumed displacement fields exactly satisfy boundary conditions at the edges. For a square plate of length/thickness equal to 5, frequencies and through-the-thickness distributions of different stress components computed with a fifth-order plate theory were found to match very well with the analytical solution of Srinivas et al. [14]. Batra and Aimmanee [15] have pointed out that both analyses and several others employing similar expansions for displacement fields missed some of the in-plane pure distortional modes that correspond to null transverse displacements. Soldatos and Hadjigergiou [16] had previously given some of these missing frequencies but did not give the corresponding mode shapes. The first few pure distortional modes of vibration and the corresponding frequencies are correctly predicted by the numerical solution of 3-dimensional elasticity equations obtained by Liew et al. [17] using the Rayleigh–Ritz method, and by Batra et al. [21] using the finite element method (FEM).

Here we use the FEM to analyze free vibrations of a thick isotropic and homogeneous plate with the Kth-order plate theory of Batra and Vidoli [8]. Since plate equations involve second-order spatial derivatives of generalized displacements, Lagrange basis functions can be used to compute the mass and the stiffness matrices. Problems with different edge conditions and aspect ratios ranging from 4 to 20 are analyzed. Results are presented for rectangular plates of different aspect ratios with edges either simply supported or clamped or two opposite edges clamped and the other two free. For simply supported plates computed frequencies and through-the-thickness distributions of transverse shear and normal stresses are found to match well with the corresponding analytical solutions. The order of the plate theory to be used for plates of different aspect ratios is also ascertained. For thin plates, the lower-order plate theories suffice to compute frequencies but not necessarily through-the-thickness variation of the transverse shear and the transverse normal stresses. For thick plates, these theories usually fail to give good values of frequencies for higher-order modes. However, higher-order plate theories give frequencies and stress distributions consistent with those obtained from the solution of three-dimensional elasticity equations.

The paper is organized as follows. Section 2 gives a brief summary of the 2-dimensional equations for a plate. The FE formulation of the problem is derived in Section 3, and results for an isotropic plate are described in Section 4. In Section 5, the present work is compared with the three-dimensional analysis of the problem by the FEM, and advantages of the former approach are stated. Section 6 outlines key differences between the present mixed higher order plate theory and other higher order plate theories. Section 7 summarizes the work and the conclusions.

2. Equations of the Kth-order plate theory

We use rectangular Cartesian coordinates, shown in Fig. 1, to describe deformations of a homogeneous plate, and denote its top, middle and bottom surfaces by S^+, S and S^- respectively. Let the length scale be normalized by $h/2$ where h is the plate thickness; thus $x_3 = +1$ on S^+ and -1 on S^-. We call the boundary $\partial S \times [-1,1]$ of the plate the mantle M or the edge surfaces, and denote the union of its upper and lower surfaces by U_B. Normal and tangential surface tractions $\mathbf{t}$

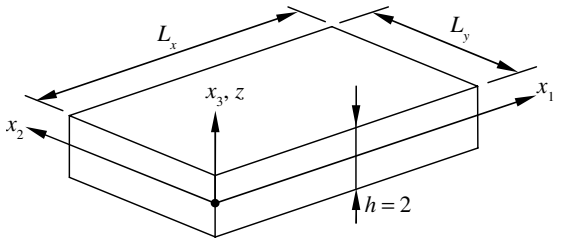

Fig. 1. Schematic sketch of the problem studied.

are prescribed on U_B, and surface tractions and/or displacements **u** on M.

Henceforth Greek indices range over 1 and 2, and Latin indices over 1, 2 and 3. We decompose as follows the position vector **x** of a point, the displacement **u**, the body force **b**, the surface traction **t**, and the outward unit normal **n**

$$x_i = x_\alpha\delta_{i\alpha} + z\delta_{i3}, \quad u_i = v_\alpha\delta_{i\alpha} + w\delta_{i3}, \quad n_i = \hat{n}_\alpha\delta_{i\alpha} + n\delta_{i3},$$
$$b_i = \hat{b}_\alpha\delta_{i\alpha} + g\delta_{i3}, \quad t_i = \hat{t}_\alpha\delta_{i\alpha} + t\delta_{i3}, \tag{1}$$

where δ_{ij} is the Kronecker delta. Thus $z = x_3$. We interchangeably use (x, y, z) and (x_1, x_2, x_3) to denote coordinates of a point. We denote partial differentiation of a variable with respect to z by a prime and with respect to x_α by a comma followed by α. The components of the infinitesimal strain tensor, e_{ij}, are given by

$$\hat{e}_{\alpha\beta} = (v_{\alpha,\beta} + v_{\beta,\alpha})/2, \quad e_{\alpha 3} \equiv \gamma_\alpha = (v'_\alpha + w_{,\alpha})/2,$$
$$e_{33} \equiv \epsilon = w'. \tag{2}$$

Thus γ_α and ϵ denote, respectively, the transverse shear strains and the transverse normal strain. Analogous to the decomposition

$$e_{ij} = \hat{e}_{\alpha\beta}\delta_{i\alpha}\delta_{j\beta} + \gamma_\alpha(\delta_{i\alpha}\delta_{j3} + \delta_{i3}\delta_{j\alpha}) + \epsilon\delta_{i3}\delta_{j3}, \tag{3}$$

of the infinitesimal strain tensor, we write the stress tensor σ_{ij} as

$$\sigma_{ij} = \hat{\sigma}_{\alpha\beta}\delta_{i\alpha}\delta_{j\beta} + \sigma^t_\alpha(\delta_{i\alpha}\delta_{j3} + \delta_{i3}\delta_{j\alpha}) + \sigma^n\delta_{i3}\delta_{j3}. \tag{4}$$

Here $\hat{\sigma}_{\alpha\beta}$, σ^t_α and σ^n signify, respectively, the in-plane components of the stress tensor, the transverse shear stresses and the transverse normal stress. The constitutive relation for an anisotropic linear elastic body is

$$\hat{e}_{\alpha\beta} = C^{pp}_{\alpha\beta\gamma\delta}\hat{\sigma}_{\gamma\delta} + C^{pt}_{\alpha\beta\gamma}\sigma^t_\gamma + C^{pn}_{\alpha\beta}\sigma^n,$$
$$\gamma_\alpha = C^{tp}_{\alpha\beta\delta}\hat{\sigma}_{\beta\delta} + C^{tt}_{\alpha\beta}\sigma^t_\beta + C^{tn}_{\alpha}\sigma^n, \tag{5}$$
$$\epsilon = C^{np}_{\alpha\beta}\hat{\sigma}_{\alpha\beta} + C^{nt}_{\beta}\sigma^t_\beta + C^{nn}\sigma^n.$$

The superscripts on **C** are not tensorial indices. When **e** and $\boldsymbol{\sigma}$ are written as $\{\hat{e}_{11}, \hat{e}_{22}, 2\hat{e}_{12}, 2\gamma_1, 2\gamma_2, \epsilon\}^{\mathrm{T}}$ and $\{\hat{\sigma}_{11}, \hat{\sigma}_{22}, \hat{\sigma}_{12}, \sigma^t_1, \sigma^t_2, \sigma^n\}^{\mathrm{T}}$, respectively, then for an isotropic material

$$\begin{Bmatrix} \hat{e}_{11} \\ \hat{e}_{22} \\ 2\hat{e}_{12} \\ 2\gamma_1 \\ 2\gamma_2 \\ \epsilon \end{Bmatrix} = \frac{1}{E}\begin{bmatrix} 1 & -\nu & 0 & 0 & 0 & -\nu \\ -\nu & 1 & 0 & 0 & 0 & -\nu \\ 0 & 0 & 2(1+\nu) & 0 & 0 & 0 \\ 0 & 0 & 0 & 2(1+\nu) & 0 & 0 \\ 0 & 0 & 0 & 0 & 2(1+\nu) & 0 \\ -\nu & -\nu & 0 & 0 & 0 & 1 \end{bmatrix} \times \begin{Bmatrix} \hat{\sigma}_{11} \\ \hat{\sigma}_{22} \\ \hat{\sigma}_{12} \\ \sigma^t_1 \\ \sigma^t_2 \\ \sigma^n \end{Bmatrix} \tag{6}$$

and

$$\mathbf{C}^{pp} = \frac{1}{E}\begin{bmatrix} 1 & -\nu & 0 \\ -\nu & 1 & 0 \\ 0 & 0 & 2(1+\nu) \end{bmatrix}, \quad \mathbf{C}^{pt} = \begin{bmatrix} 0 & 0 \\ 0 & 0 \\ 0 & 0 \end{bmatrix},$$
$$\mathbf{C}^{pn} = \frac{1}{E}\begin{Bmatrix} -\nu \\ -\nu \\ 0 \end{Bmatrix},$$
$$\mathbf{C}^{tp} = \begin{bmatrix} 0 & 0 & 0 \\ 0 & 0 & 0 \end{bmatrix}, \quad \mathbf{C}^{tt} = \frac{1}{E}\begin{bmatrix} 2(1+\nu) & 0 \\ 0 & 2(1+\nu) \end{bmatrix},$$
$$\mathbf{C}^{tn} = \begin{Bmatrix} 0 \\ 0 \end{Bmatrix},$$
$$\mathbf{C}^{np} = \frac{1}{E}[-\nu \quad -\nu \quad 0], \quad \mathbf{C}^{nt} = [0 \quad 0], \quad \mathbf{C}^{nn} = \frac{1}{E}[1]. \tag{7}$$

Here E is Young's modulus and ν Poisson's ratio. Expressions for matrices in (5) for transversely isotropic and orthotropic materials are given in Appendix A.

Batra and Vidoli [8] used a mixed variational principle of Yang and Batra [23] to derive a higher-order theory for piezoelectric plates. Batra et al. [13] employed the Hellinger–Reissner principle to deduce the corresponding higher-order mechanical theory for anisotropic plates. When using a mixed variational principle, one postulates independently expressions for displacements and stresses. We use orthonormal Legendre polynomials $L_0(z), L_1(z), \ldots, L_K(z)$ defined on $[-1, 1]$ and satisfying

$$\int_{-1}^{1} L_a(z)L_b(z)\mathrm{d}z = \delta_{ab}, \quad a, b = 0, 1, 2, \ldots, K, \tag{8}$$

as the basis functions to expand displacements and stresses in powers of z. Henceforth, unless stated otherwise, indices a and b will range over 0,1,2, …, K. Also, a repeated index is summed irrespective of its appearance as a subscript or a superscript or its being enclosed in parentheses. Note that

$$\begin{aligned}
&L_0(z)=\frac{1}{\sqrt{2}},\quad L_1(z)=\sqrt{\frac{3}{2}}z,\quad L_2(z)=\sqrt{\frac{5}{2}}\frac{(3z^2-1)}{2},\\
&L_3(z)=\sqrt{\frac{7}{2}}\frac{(-3z+5z^3)}{2},\quad L_4(z)=\frac{3}{8\sqrt{2}}(3-30z^2+35z^4),\\
&L_5(z)=\frac{1}{8}\sqrt{\frac{11}{2}}(15z-70z^3+63z^5),\\
&L_6(z)=\frac{1}{16}\sqrt{\frac{13}{2}}(-5+105z^2-315z^4+231z^6),\\
&L_7(z)=\frac{1}{16}\sqrt{\frac{15}{2}}(-35z+315z^3-639z^5+429z^7),\ldots
\end{aligned}\tag{9}$$

and

$$L'_a(z)=\sum_{b=1}^{(a-1)}D_{ab}L_b(z),\tag{10}$$

where D_{ab} are constants. For the Kth order plate theory, $D_{aK}=D_{Ka}=0$, $a=0,1,2,\ldots,K$. For $K=7$

$$[D]=\begin{pmatrix}
0 & 0 & 0 & 0 & 0 & 0 & 0 & 0\\
\sqrt{3} & 0 & 0 & 0 & 0 & 0 & 0 & 0\\
0 & \sqrt{15} & 0 & 0 & 0 & 0 & 0 & 0\\
\sqrt{7} & 0 & \sqrt{35} & 0 & 0 & 0 & 0 & 0\\
0 & 3\sqrt{3} & 0 & 3\sqrt{7} & 0 & 0 & 0 & 0\\
\sqrt{11} & 0 & \sqrt{55} & 0 & 3\sqrt{13} & 0 & 0 & 0\\
0 & \sqrt{39} & 0 & \sqrt{91} & 0 & \sqrt{143} & 0 & 0\\
\sqrt{15} & 0 & 5\sqrt{3} & 0 & 3\sqrt{15} & 0 & \sqrt{195} & 0
\end{pmatrix}.\tag{11}$$

We set

$$\begin{aligned}
v_\alpha(x_\beta,z,t)&=L_a(z)v_\alpha^{(a)}(x_\beta,t),\\
w(x_\beta,z,t)&=L_a(z)w^{(a)}(x_\beta,t),\\
\hat{\sigma}_{\alpha\beta}(x_\gamma,z,t)&=L_a(z)N_{\alpha\beta}^{(a)}(x_\gamma,t),\\
\sigma_\alpha^t(x_\gamma,z,t)&=\widetilde{L}_a(z)T_\alpha^{(a)}(x_\gamma,t)+\alpha_0[L_0(z)-\widetilde{L}_0(z)]\hat{t}_\alpha^{(0)}(x_\gamma,t)\\
&\quad+\alpha_1[L_1(z)-\tilde{L}_1(z)]\hat{t}_\alpha^{(1)}(x_\gamma,t),\\
\sigma^n(x_\gamma,z,t)&=\widetilde{L}_a(z)\Sigma^{(a)}(x_\gamma,t)+\alpha_0[L_0(z)-\widetilde{L}_0(z)]t^{(0)}(x_\gamma,t)\\
&\quad+\alpha_1[L_1(z)-\widetilde{L}_1(z)]t^{(1)}(x_\gamma,t),
\end{aligned}\tag{12}$$

where

$$\begin{aligned}
&\hat{t}_\alpha^{(0)}=(\hat{t}_\alpha^{+}-\hat{t}_\alpha^{-})/2,\quad \hat{t}_\alpha^{(1)}=(\hat{t}_\alpha^{+}+\hat{t}_\alpha^{-})/2,\\
&t^{(0)}=(t^{+}-t^{-})/2,\quad t^{(1)}=(t^{+}+t^{-})/2,\\
&\alpha_0=1/L_0(1),\quad \alpha_1=1/L_1(1),\\
&\int_{-1}^{1}\widetilde{L}_a(z)L_b(z)\mathrm{d}z=\delta_{ab},\quad \widetilde{L}_a(\pm1)=0.
\end{aligned}\tag{13}$$

Here t^+ and t^- are the normal tractions (pressures) and $\hat{\mathbf{t}}^+$ and $\hat{\mathbf{t}}^-$ are the tangential tractions applied, respectively, on the top and the bottom surfaces of the plate. $N_{\alpha\beta}^{(a)}=N_{\beta\alpha}^{(a)}$. $N_{\alpha\beta}^{(0)}$ is the membranal stress tensor, $N_{\alpha\beta}^{(1)}$ is the matrix of bending moments, and matrices $N_{\alpha\beta}^{(a)}$ $(a=2,3,\ldots,K)$ are comprised of a linear combination of matrices of bending moments of order zero through a. $T_\alpha^{(0)}$ is the resultant shear force, $T_\alpha^{(1)}$ is the moment of internal double forces acting along the x_3-axis, and $T_\alpha^{(a)}$ equals the linear combination of moments up to the ath order of the internal double forces. $\Sigma^{(0)}$ is the transverse normal force, and $\Sigma^{(a)}$ the linear combination of moments up to the ath order of the transverse normal force. The function $\widetilde{L}_a(z)$ is a modified Legendre polynomial of degree $K+2$ that is orthogonal to the K Legendre polynomials $L_b(z)$ for $a\neq b$, and also vanishes at $z=\pm1$. Thus traction boundary conditions prescribed on S^+ and S^- are exactly satisfied by $(12)_{4-5}$. For $K=3$

$$\begin{aligned}
\widetilde{L}_0(z)&=\frac{\sqrt{2}}{16}(5+30z^2-35z^4),\\
\widetilde{L}_1(z)&=\frac{1}{16}\sqrt{\frac{2}{3}}(-21z+210z^3-189z^5),\\
\widetilde{L}_2(z)&=\frac{1}{16}\sqrt{\frac{2}{5}}(-35+210z^2-175z^4),\\
\widetilde{L}_3(z)&=\frac{1}{16}\sqrt{\frac{2}{7}}(-187z+630z^3-441z^5).
\end{aligned}\tag{14}$$

Note that expressions for the modified Legendre polynomials depend upon the order K of the plate theory. For example, for $K=7$, $\widetilde{L}_0(z)$, $\widetilde{L}_1(z)$, $\widetilde{L}_2(z)$ and $\widetilde{L}_3(z)$ listed in Appendix B differ from those given in (14) because functions in (14) are orthogonal to L_0, L_1, L_2 and L_3, and those in Appendix B are orthogonal to $L_0, L_1, L_2, \ldots, L_7$.

Recalling (9), (12) and (14), we see that for a Kth order plate theory, the three components of displacements and the three components of the inplane stress tensor are expanded in z upto powers of z^K. However, the transverse stresses are expanded in z upto powers of z^{K+2}. This is permissible in a plate theory derived from a mixed variational principle. Basis functions $L_0(z), L_1(z), L_2(z), \ldots$ are equivalent to $1, z, z^2, \ldots$. An advantage of using $L_0(z), L_1(z) \ldots$ is that they are mutually orthogonal on $[-1,1]$ and the algebraic work is reduced. For example, the mass matrix R_{ab} appearing in the equations of motion (17) is diagonal for Legendre polynomials as basis functions and nondiagonal when $1, z, z^2, \ldots$ are used as basis functions. By a suitable identification of the generalized displacements one can deduce the classical plate theory, the first-order shear deformation theory, and the third-order shear deformation theory.

Substitution for v_α and w from $(12)_1$ and $(12)_2$ into (2) and setting

$$\begin{aligned}
&\hat{e}_{\alpha\beta}(x_\gamma, z, t) = L_a(z)\hat{e}^{(a)}_{\alpha\beta}(x_\gamma, t),\\
&\gamma_\alpha(x_\beta, z, t) = L_a(z)\gamma^{(a)}_\alpha(x_\beta, t),\\
&\epsilon(x_\beta, z, t) = L_a(z)\epsilon^{(a)}(x_\beta, t),
\end{aligned} \tag{15}$$

we obtain

$$\begin{aligned}
&\hat{e}^{(a)}_{\alpha\beta} = (v^{(a)}_{\alpha,\beta} + v^{(a)}_{\beta,\alpha})/2,\\
&2\gamma^{(a)}_\alpha = w^{(a)}_{,\alpha} + D_{ab}v^{(b)}_\alpha,\\
&\epsilon^{(a)} = D_{ab}w^{(b)}.
\end{aligned} \tag{16}$$

Omitting details which can be found in Refs. [8,13] we give below the balance laws, constitutive relations, boundary conditions and initial conditions for the 2-dimensional Kth-order mixed shear and normal deformable theory for a homogeneous plate.

Balance laws

$$\begin{aligned}
&N^{(a)}_{\alpha\beta,\beta} - D_{ab}T^{(b)}_\alpha + B^{(a)}_\alpha = R_{ab}\ddot{v}^{(b)}_\alpha \text{ on } S,\\
&\qquad a = 0, 1, 2, \ldots, K; \quad \alpha = 1, 2;\\
&T^{(a)}_{\alpha,\alpha} - D_{ab}\Sigma^{(b)} + \Gamma^{(a)} = R_{ab}\ddot{w}^{(b)} \text{ on } S.
\end{aligned} \tag{17}$$

Constitutive relations

$$\begin{aligned}
\hat{e}^{(a)}_{\alpha\beta} &= C^{pp}_{\alpha\beta\gamma\delta}N^{(a)}_{\gamma\delta} + C^{pt}_{\alpha\beta\gamma}T^{(a)}_\gamma + C^{pn}_{\alpha\beta}\Sigma^{(a)},\\
\gamma^{(a)}_\alpha &= C^{tp}_{\alpha\beta\delta}N^{(a)}_{\beta\delta} + C^{tt}_{\alpha\beta}P_{ab}T^{(b)}_\beta + C^{tn}_\alpha P_{ab}\Sigma^{(b)}\\
&\quad + (\delta_{ab} - P_{ab})\alpha_b(C^{tt}_{\alpha\beta}\hat{t}^{(a)}_\beta + C^{tn}_\alpha t^{(a)}),\\
\epsilon^{(a)} &= C^{np}_{\alpha\beta}N^{(a)}_{\alpha\beta} + C^{nt}_\beta P_{ab}T^{(b)}_\beta + C^{nn}P_{ab}\Sigma^{(b)}\\
&\quad + (\delta_{ab} - P_{ab})\alpha_b(C^{nt}_\alpha\hat{t}^{(a)}_\alpha + C^{nn}t^{(a)}).
\end{aligned} \tag{18}$$

Boundary conditions

$$\begin{aligned}
&N^{(a)}_{\alpha\beta}\hat{n}_\beta = F^{(a)}_\alpha,\ T^{(a)}_\alpha n_\alpha = F^{(a)}_3 \text{ on } \partial_t S,\\
&v^{(a)}_\alpha = \tilde{v}^{(a)}_\alpha,\ w^{(a)} = \tilde{w}^{(a)} \text{ on } \partial_u S.
\end{aligned} \tag{19}$$

Initial conditions

$$\begin{aligned}
&v^{(a)}_\alpha(x_\beta, 0) = \overset{\circ}{v}{}^{(a)}_\alpha(x_\beta),\\
&w^{(a)}_\alpha(x_\beta, 0) = \overset{\circ}{w}{}^{(a)}_\alpha(x_\beta).
\end{aligned} \tag{20}$$

Here

$$\begin{aligned}
B^{(a)}_\alpha &= \int_{-1}^{1} L_a\hat{b}_\alpha\,\mathrm{d}z + L_a(1)\hat{t}^+_\alpha + L_a(-1)\hat{t}^-_\alpha,\\
\Gamma^{(a)} &= \int_{-1}^{1} L_a g\,\mathrm{d}z + L_a(1)t^+ + L_a(-1)t^-,\\
R_{ab} &= \int_{-1}^{1} \rho L_a L_b\,\mathrm{d}z = \rho\delta_{ab},\ P_{ab} = \int_{-1}^{1} \widetilde{L}_a\widetilde{L}_b\,\mathrm{d}z,
\end{aligned} \tag{21}$$

and $\partial_t S$ and $\partial_u S$ are parts of the boundary ∂S of S where surface tractions and displacements are prescribed respectively. In the fourth term on the right-hand side of equations $(18)_2$ and $(18)_3$, the repeated index a is not summed but b is summed. Also $\hat{\mathbf{t}}^{(2)} = \hat{\mathbf{t}}^{(3)} = \cdots = \hat{\mathbf{t}}^{(K)} = \mathbf{0}$, $t^{(2)} = t^{(3)} = \ldots = t^{(K)} = 0$. The presence of the matrix P_{ab} in equations $(18)_2$ and $(18)_3$ implies that $\boldsymbol{\gamma}^{(a)}$ and $\epsilon^{(a)}$ depend upon $\mathbf{T}^{(b)}$ and $\Sigma^{(b)}$ for $0 \leqslant b \leqslant K$. Thus equations for the transverse strains and moments of transverse forces are strongly coupled. Because of the presence of $\mathbf{T}^{(a)}$ in equations $(17)_1$ and $(17)_2$, these two equations are coupled. Also, the occurrence of D_{ab} in $(17)_1$ implies that equations for $a = K$ involve $\mathbf{T}^{(0)}, \mathbf{T}^{(1)}, \ldots, \mathbf{T}^{(K-1)}$. These comments should become transparent from the explicit forms of equations (17) given in Appendix C.

For $a = 0, 1, 2, \ldots, K$, using equations (16), strains on the left hand side of equations (18) are replaced by gradients of displacements, the resulting equations solved for $\mathbf{N}^{(a)}$, $\mathbf{T}^{(a)}$ and $\Sigma^{(a)}$ in terms of displacement gradients (e.g. see Appendix C), and the result substituted into equations (17). We thus obtain second-order partial differential equations for displacements $\mathbf{v}^{(a)}$ and $w^{(a)}$ defined on the midsurface S. These equations under boundary conditions (19) and initial conditions (20) are solved for $\mathbf{v}^{(a)}$ and $w^{(a)}$. Stresses $\hat{\boldsymbol{\sigma}}$, $\boldsymbol{\sigma}^t$ and σ^n are computed from Eqs. $(12)_{3-5}$, (16) and (18).

For $K = 0$, the present plate theory reduces essentially to a membrane theory. For $K = 1$, we get a modified FSDT (first-order shear deformation theory) in which the transverse normal strain is a constant, the transverse normal and shear stresses are polynomials in z of degree at most 3, and surface tractions on the top and the bottom surfaces of the plate are exactly satisfied. For $K = 3$, we get a modified TSDT (third-order shear deformation theory) with the transverse normal strain varying quadratically through the plate thickness, the transverse normal and shear stresses polynomials in z of degree at most 5, and surface tractions on the top and the bottom surfaces exactly satisfied. Whereas in a plate theory derived from a mixed variational principle, one can assume that the transverse strains and stresses may be represented by polynomials of different order of z, in the compatible plate theory such is not the case. In the later case, expressions for stresses are deduced by substituting in the constitutive relation (5) the expressions for strains. Thus expressions for stresses and strains have expansions of the same order in z. However, traction boundary conditions on the top and the bottom surfaces of the plate are not necessarily satisfied. Because of the higher-order expansions for transverse stresses in the mixed plate theory, higher order moments of transverse stresses appear in the two-dimensional balance laws of the plate theory. The expectation is that the exact satisfaction of traction boundary conditions on the top and the bottom surfaces will give results in better agreement with those obtained from the 3-dimensional elasticity theory than those computed from the compatible plate theory. We also note that three-dimensional analytical solutions [19] reveal that for thick laminates, the plate thickness changes and

through-the-thickness variation of the transverse shear stress can not be described by a polynomial of degree 2 or higher in z. The smallest value of K for which the plate theory accurately predicts stresses and displacements depends upon the aspect ratio of the plate, symmetries of its material, the boundary conditions and the loads applied.

For simply supported (SP), clamped (C) and free (F) edges of the plate, boundary conditions (19) become

$$\begin{aligned}\text{SP}: N_{11}^{(a)} = 0, \quad w^{(a)} = 0, \quad v_2^{(a)} = 0, \quad \text{on } x_1 = 0, L_x,\\ N_{22}^{(a)} = 0, \quad w^{(a)} = 0, \quad v_1^{(a)} = 0, \quad \text{on } x_2 = 0, L_y;\end{aligned} \tag{22}$$

$$\text{C}: v_1^{(a)} = v_2^{(a)} = w^{(a)} = 0, \quad \text{on } x_1 = 0, L_x,\ x_2 = 0, L_y; \tag{23}$$

$$\begin{aligned}\text{F}: N_{11}^{(a)} = 0, \quad N_{21}^{(a)} = 0, \quad T_1^{(a)} = 0 \quad \text{on } x_1 = 0, L_x,\\ N_{12}^{(a)} = 0, \quad N_{22}^{(a)} = 0, \quad T_2^{(a)} = 0 \quad \text{on } x_2 = 0, L_y.\end{aligned} \tag{24}$$

Boundary conditions (22) are analogous to those used by Srinivas et al. [14] at a simply supported edge. These do not simulate well conditions used in a laboratory where a plate edge is supported either on a knife edge or on a hemispherical edge.

3. Weak formulation of equations of the plate theory

For $a = 0,1,2,\ldots,K$, a weak formulation of Eqs. (17)–(20) is derived. Let $\phi_\alpha^{(a)}$ and $\phi_3^{(a)}$, $a = 0,1,2,\ldots,K$ be smooth test functions that vanish on $\partial_u S$ where $v_\alpha^{(a)}$ and $w^{(a)}$ are specified. Taking the inner product of Eq. $(17)_1$ with $\phi_\alpha^{(a)}$ and of equation $(17)_2$ with $\phi_3^{(a)}$, integrating the resulting equations over S, using the divergence theorem on the first term on the left-hand side of each equation, and using the natural boundary conditions $(19)_1$, we obtain

$$\begin{aligned}&\int_S R_{ab}\ddot{v}_\alpha^{(b)}\phi_\alpha^{(a)}\,\mathrm{d}\Omega + \int_S N_{\alpha\beta}^{(a)}\phi_{\alpha,\beta}^{(a)}\,\mathrm{d}\Omega + \int_S D_{ab}T_\alpha^{(b)}\phi_\alpha^{(a)}\,\mathrm{d}\Omega\\ &\quad = \int_S B_\alpha^{(a)}\phi_\alpha^{(a)}\mathrm{d}\Omega + \int_{\partial_t S} F_\alpha^{(a)}\phi_\alpha^{(a)}\mathrm{d}\Omega,\\ &\int_S R_{ab}\ddot{w}^{(b)}\phi_3^{(a)}\mathrm{d}\Omega + \int_S T_\alpha^{(a)}\phi_{3,\alpha}^{(a)}\mathrm{d}\Omega + \int_S D_{ab}\Sigma^{(b)}\phi_3^{(a)}\mathrm{d}\Omega\\ &\quad = \int_S \Gamma^{(a)}\phi_3^{(a)}\,\mathrm{d}\Omega + \int_{\partial_t S} F_3^{(a)}\phi_3^{(a)}\,\mathrm{d}\Gamma.\end{aligned} \tag{25}$$

Eqs. (18) are solved for $\mathbf{N}^{(a)}$, $\mathbf{T}^{(a)}$ and $\Sigma^{(a)}$ in terms of $\hat{\mathbf{e}}^{(a)}$, $\boldsymbol{\gamma}^{(a)}$, $\epsilon^{(a)}$, $\hat{\mathbf{t}}^{(a)}$ and $t^{(a)}$ with the following result:

$$\begin{aligned}N_{\alpha\beta}^{(a)} &= E_{\alpha\beta\gamma\delta}^{pp}\hat{e}_{\gamma\delta}^{(a)} + E_{\alpha\beta\delta}^{pt}\gamma_\delta^{(a)} + E_{\alpha\beta}^{pn}\epsilon^{(a)} + \widetilde{E}_{\alpha\beta\gamma}^{pt}\hat{t}_\gamma^{(a)} + \widetilde{E}_{\alpha\beta}^{pn}t^{(a)},\\ T_\alpha^{(a)} &= E_{\alpha\beta\gamma}^{tp}\hat{e}_{\beta\gamma}^{(a)} + E_{\alpha\beta}^{tt}\widetilde{P}_{ab}\gamma_\beta^{(b)} + E_\alpha^{tn}\widetilde{Q}_{ab}\epsilon^{(b)}\\ &\quad + \overline{P}_{ab}(\widetilde{E}_{\alpha\beta}^{tt}\hat{t}_\beta^{(b)} + \widetilde{E}^{tn}t^{(b)}),\\ \Sigma^{(a)} &= E_{\alpha\beta}^{np}\hat{e}_{\alpha\beta}^{(a)} + E_\alpha^{nt}\widehat{P}_{ab}\gamma_\alpha^{(a)} + E^{nn}\widehat{Q}_{ab}\epsilon^{(b)}\\ &\quad + \overline{P}_{ab}(\widetilde{E}_\alpha^{nt}\hat{t}_\alpha^{(b)} + \widetilde{E}^{nn}t^{(b)}).\end{aligned} \tag{26}$$

Matrices $\widetilde{P}_{ab}$, $\widehat{P}_{ab}$, $\overline{P}_{ab}$, $\widetilde{Q}_{ab}$ and $\widehat{Q}_{ab}$ provide coupling among $(\mathbf{T}^{(a)}, \Sigma^{(a)})$ and $(\boldsymbol{\gamma}^{(0)}, \epsilon^{(0)}, \boldsymbol{\gamma}^{(1)}, \epsilon^{(1)}, \ldots, \boldsymbol{\gamma}^{(a)}, \epsilon^{(a)})$. We rewrite Eqs. (26) as

$$\begin{Bmatrix} N_{11}^{(a)} \\ N_{22}^{(a)} \\ N_{12}^{(a)} \\ T_1^{(a)} \\ T_2^{(a)} \\ \Sigma^{(a)} \end{Bmatrix} = \sum_{b=0}^{a} \left(\begin{bmatrix} \mathbf{E}_b^{pp} & \mathbf{E}_b^{pt} & \mathbf{E}_b^{pn} \\ \mathbf{E}_b^{tp} & \mathbf{E}_b^{tt} & \mathbf{E}_b^{tn} \\ \mathbf{E}_b^{np} & \mathbf{E}_b^{nt} & \mathbf{E}_b^{nn} \end{bmatrix} \begin{Bmatrix} \hat{e}_{11}^{(b)} \\ \hat{e}_{22}^{(b)} \\ 2\hat{e}_{12}^{(b)} \\ 2\gamma_1^{(b)} \\ 2\gamma_2^{(b)} \\ \epsilon^{(b)} \end{Bmatrix} + \begin{bmatrix} \widetilde{\mathbf{E}}_b^{pt} & \widetilde{\mathbf{E}}_b^{pn} \\ \widetilde{\mathbf{E}}_b^{tt} & \widetilde{\mathbf{E}}_b^{tn} \\ \widetilde{\mathbf{E}}_b^{nt} & \widetilde{\mathbf{E}}_b^{nn} \end{bmatrix} \begin{Bmatrix} \hat{t}_1^{(b)} \\ \hat{t}_2^{(b)} \\ \hat{t}^{(b)} \end{Bmatrix} \right). \tag{27}$$

For a traction free plate made of a homogeneous and isotropic material, Appendix C lists Eqs. (27) for $K = 1$, 3 and 5.

In order to solve the problem by the FEM, we divide the midsurface S into disjoint quadrilaterals (or triangles) and select an appropriate number of nodes, N_d, on each element S_e. On S_e, we approximate displacements by

$$\begin{aligned}&v_\alpha^{(a)}(x_\beta, t) = \psi_A(x_\beta)d_{A\alpha}^{(a)}(t),\\ &w^{(a)}(x_\beta, t) = \psi_A(x_\beta)d_{A3}^{(a)}(t),\\ &A = 1,2,\ldots,N_d,\\ &\phi_\alpha^{(a)}(x_\beta) = \psi_A(x_\beta)\widetilde{C}_{A\alpha}^{(a)},\\ &\phi_3^{(a)}(x_\beta) = \psi_A(x_\beta)\widetilde{C}_{A3}^{(a)},\end{aligned} \tag{28}$$

where $\psi_1(x_\beta)$, $\psi_2(x_\beta)$, $\ldots$, $\psi_{N_d}(x_\beta)$ are the FE shape functions, $d_{A\alpha}^{(a)}$ and $d_{A3}^{(a)}$ are the time-dependent nodal displacements, $\widetilde{C}_{A\alpha}^{(a)}$ and $\widetilde{C}_{A3}^{(a)}$ are constants defining test functions $\phi_\alpha^{(a)}$ and $\phi_3^{(a)}$, and the index A is summed. For a Kth order plate theory, there are $3(K+1)$ unknown $\mathbf{d}$'s at each node. For each value of a, strains are computed from

$$
\begin{aligned}
2\hat{e}^{(a)}_{\alpha\beta} &= \psi_{A,\alpha} d^{(a)}_{A\beta} + \psi_{A,\beta} d^{(a)}_{A\alpha},\\
2\gamma^{(a)}_{1} &= \psi_{A,1} d^{(a)}_{A3} + D_{ab}\psi_A d^{(b)}_{A1},\\
2\gamma^{(a)}_{2} &= \psi_{A,2} d^{(a)}_{A3} + D_{ab}\psi_A d^{(b)}_{A2},\\
\epsilon^{(a)} &= D_{ab}\psi_A d^{(b)}_{A3},
\end{aligned}
\tag{29}
$$

where $\psi_{A,\alpha} = \partial\psi_A/\partial x_\alpha$. Whereas the ath order in-plane strains $\hat{e}^{(a)}_{\alpha\beta}$ depend only upon the ath order nodal displacements $\mathbf{d}^{(a)}$, ath order transverse shear and normal strains depend upon nodal displacements $\mathbf{d}^{(0)}, \mathbf{d}^{(1)}, \ldots, \mathbf{d}^{(a)}$. Eqs. (29) can be written as

$$
\{\mathrm{e}^{(a)}\} = \sum_{b=0}^{a} ([B^{(ab)}]\{d^{(b)}\}), \tag{30}
$$

where $\{e^{(a)}\}$, $[B^{(ab)}]$ and $\{d^{(a)}\}$ are 6×1, 6×12 and 12×1 matrices for a 4-node quadrilateral element. Furthermore, for $a = b$

$$
[B^{(ab)}] = \begin{bmatrix}
\frac{\partial\psi_1}{\partial x_1} & 0 & 0 & \frac{\partial\psi_2}{\partial x_1} & 0 & 0 & \frac{\partial\psi_3}{\partial x_1} & 0 & 0 & \frac{\partial\psi_4}{\partial x_1} & 0 & 0\\
0 & \frac{\partial\psi_1}{\partial x_2} & 0 & 0 & \frac{\partial\psi_2}{\partial x_2} & 0 & 0 & \frac{\partial\psi_3}{\partial x_2} & 0 & 0 & \frac{\partial\psi_4}{\partial x_2} & 0\\
\frac{\partial\psi_1}{\partial x_2} & \frac{\partial\psi_1}{\partial x_1} & 0 & \frac{\partial\psi_2}{\partial x_2} & \frac{\partial\psi_2}{\partial x_1} & 0 & \frac{\partial\psi_3}{\partial x_2} & \frac{\partial\psi_3}{\partial x_1} & 0 & \frac{\partial\psi_4}{\partial x_2} & \frac{\partial\psi_4}{\partial x_1} & 0\\
0 & 0 & \frac{\partial\psi_1}{\partial x_1} & 0 & 0 & \frac{\partial\psi_2}{\partial x_1} & 0 & 0 & \frac{\partial\psi_3}{\partial x_1} & 0 & 0 & \frac{\partial\psi_4}{\partial x_1}\\
0 & 0 & \frac{\partial\psi_1}{\partial x_2} & 0 & 0 & \frac{\partial\psi_2}{\partial x_2} & 0 & 0 & \frac{\partial\psi_3}{\partial x_2} & 0 & 0 & \frac{\partial\psi_4}{\partial x_2}\\
0 & 0 & 0 & 0 & 0 & 0 & 0 & 0 & 0 & 0 & 0 & 0
\end{bmatrix}
$$

and for $a \neq b$

$$
[B^{(ab)}] = \begin{bmatrix}
0 & 0 & 0 & 0 & 0 & 0 & 0 & 0 & 0 & 0 & 0 & 0\\
0 & 0 & 0 & 0 & 0 & 0 & 0 & 0 & 0 & 0 & 0 & 0\\
0 & 0 & 0 & 0 & 0 & 0 & 0 & 0 & 0 & 0 & 0 & 0\\
D_{ab}\psi_1 & 0 & 0 & D_{ab}\psi_2 & 0 & 0 & D_{ab}\psi_3 & 0 & 0 & D_{ab}\psi_4 & 0 & 0\\
0 & D_{ab}\psi_1 & 0 & 0 & D_{ab}\psi_2 & 0 & 0 & D_{ab}\psi_3 & 0 & 0 & D_{ab}\psi_4 & 0\\
0 & 0 & D_{ab}\psi_1 & 0 & 0 & D_{ab}\psi_2 & 0 & 0 & D_{ab}\psi_3 & 0 & 0 & D_{ab}\psi_4
\end{bmatrix}
\tag{31}
$$

where $[d^{(a)}]^{\mathrm{T}} = \{d^{(a)}_{11}\ d^{(a)}_{12}\ d^{(a)}_{13}\ d^{(a)}_{21}\ d^{(a)}_{22}\ d^{(a)}_{23}\ d^{(a)}_{31}\ d^{(a)}_{32}\ d^{(a)}_{33}\ d^{(a)}_{41}\ d^{(a)}_{42}\ d^{(a)}_{43}\}$. The first index on $d^{(a)}_{11}$ indicates the local node number and the second index the coordinate axis. When Eq. (30) is written in the more familiar form as

$$
\{e\} = [B]\{d\} \tag{32}
$$

then for a Kth-order plate theory $\{e\}$ is a 6×1 matrix, $[B]$ a $6\times 3(K+1)N^e_n$ matrix and $\{d\}$ a $(3K+1)N^e_n$ column matrix where N^e_n equals the number of nodes in an element.

Substituting from (28)–(32) into (25) and exploiting the fact that the resulting equation must hold for all choices of constants $\mathbf{C}$ in (28), we obtain

$$
\mathbf{M}\ddot{\mathbf{d}} + \mathbf{K}\mathbf{d} = \mathbf{F}, \tag{33}
$$

where $\mathbf{M}$, $\mathbf{K}$ and $\mathbf{F}$ are, respectively, the mass matrix, the stiffness matrix and the load vector. Square matrices M and $\mathbf{K}$ have $3(K+1)N_n$ rows, and the column matrix $\mathbf{F}$ has $3(K+1)N_n$ rows, where N_n is the number of nodes in the FE mesh. We note that the natural or traction boundary conditions are already included in (33). Essential or displacement boundary conditions are imposed after equations (33) have been written as algebraic equations by using a time-integration scheme. Initial values of nodal displacements are deduced from equations (20).

For a free vibration problem

$$
\mathbf{F} = \mathbf{0},\ \mathbf{d}(t) = \mathbf{D}\mathrm{e}^{i\omega t}, \tag{34}
$$

where ω is a natural frequency. In this case, no initial conditions are needed. Eqs. (33) and (34) yield

$$
(\mathbf{K} - \omega^2\mathbf{M})\mathbf{D} = \mathbf{0}. \tag{35}
$$

Matrices $\mathbf{M}$ and $\mathbf{K}$ are modified to satisfy the prescribed essential boundary conditions, and then frequencies ω are computed by solving the algebraic equation

$$
\det[\mathbf{K} - \omega^2\mathbf{M}] = 0. \tag{36}
$$

The mode shape corresponding to the frequency ω is obtained by deleting one of the equations in (35) that does not enforce the essential boundary conditions and replacing it with a suitable normalization condition.

4. Computation and discussion of results

We have developed an FE code based on the formulation described in Section 3 and employing 4-node isoparametric quadrilateral elements, consistent mass matrix and 2×2 integration rule to evaluate various integrals appearing in the weak formulation of the problem. Table 1 lists the lowest ten computed and analytical frequencies of a simply supported rectangular plate with $L_x/L_y = 2$ and $L_x/h = 4,8,12$ and 20. The first column in Table 1 also lists whether the mode shape corresponds to deformations that are symmetric (s) or antisymmetric (a) about the midsurface of the plate. The two numbers (m,n) following (s) or (a) give values of m and n in the displacement field:

Table 1
Comparison of first ten nondimensional frequencies of a simply supported rectangular plate ($L_x = 2L_y$) with the exact solution of Srinivas et al. [14]

Mode	Present plate theory $K = 5$	Exact	% Error
(a) $L_x/h = 4; K = 5$			
1(*s*)(1,0)	0.7857	0.7854	−0.0438
2(*a*)(1,1)	1.0725	1.0692	−0.3087
3(*a*)(2,1)	1.5248	1.5158	−0.5904
4(*s*)(0,1)	1.5715	1.5708	−0.0442
4(*s*)(2,0)	1.5763	1.5708	−0.3520
5(*s*)(1,1)	1.7587	1.7562	−0.1428
6(*a*)(3,1)	2.1500	2.1219	−1.3245
7(*s*)(2,1)	2.2343	2.2214	−0.5799
8(*s*)(3,0)	2.3766	2.3562	−0.8667
9(*a*)(1,2)	2.5490	2.5305	−0.7312
10(*a*)(2,2)	2.8263	2.8066	−0.7011
10(*a*)(4,1)	2.8721	2.8066	−2.3346
(b) $L_x/h = 8; K = 5$			
1(*a*)(1,1)	0.3349	0.3373	−0.7210
2(*s*)(1,0)	0.3927	0.3929	−0.0540
3(*a*)(2,1)	0.5066	0.5131	−1.2771
4(*a*)(3,1)	0.7606	0.7800	−2.5520
5(*s*)(0,1)	0.7854	0.7858	−0.0546
5(*s*)(2,0)	0.7854	0.7888	−0.4344
6(*s*)(1,1)	0.8781	0.8797	−0.1765
7(*a*)(1,2)	0.9425	0.9550	−1.3247
8(*a*)(2,2)	1.0692	1.0823	−1.2258
8(*a*)(4,1)	1.0692	1.1131	−4.1036
9(*s*)(2,1)	1.1107	1.1187	−0.7164
10(*s*)(3,0)	1.1781	1.1907	−1.0700
	Present plate theory $K = 3$	Exact	% Error
(c) $L_x/h = 12; K = 3$			
1(*a*)(1,1)	0.1594	0.1581	−0.8450
2(*a*)(2,1)	0.2490	0.2455	−1.4096
3(*s*)(1,0)	0.2619	0.2618	−0.0277
4(*a*)(3,1)	0.3913	0.3811	−2.6698
5(*a*)(1,2)	0.4887	0.4822	−1.3401
6(*s*)(0,1)	0.5237	0.5236	−0.0279
6(*s*)(2,0)	0.5248	0.5236	−0.2250
7(*a*)(2,2)	0.5611	0.5544	−1.2124
7(*a*)(4,1)	0.5768	0.5544	−4.0440
8(*s*)(1,1)	0.5859	0.5854	−0.0906
9(*a*)(3,2)	0.6787	0.6686	−1.5044
10(*s*)(2,1)	0.7432	0.7405	−0.3646
(d) $L_x/h = 20; K = 3$			
1(*a*)(1,1)	0.0601	0.0589	−2.0806
2(*a*)(2,1)	0.0962	0.0931	−3.2489
3(*a*)(3,1)	0.1567	0.1485	−5.5275
4(*s*)(1,0)	0.1571	0.1571	−0.0150
5(*a*)(1,2)	0.1963	0.1913	−2.6252
6(*a*)(2,2)	0.2279	0.2226	−2.3759
6(*a*)(4,1)	0.2399	0.2226	−7.7908
7(*a*)(3,2)	0.2812	0.2735	−2.8269
8(*a*)(5,1)	0.3438	0.313	−9.8495
9(*s*)(0,1)	0.3142	0.3142	−0.0151
9(*s*)(2,0)	0.3149	0.3142	−0.2122
10(*a*)(4,2)	0.3560	0.3421	−4.0698

$$u_1 = e^{i\omega t} U_1(x_3) \cos\frac{m\pi x_1}{L_x} \sin\frac{n\pi x_2}{L_y},$$
$$u_2 = e^{i\omega t} U_2(x_3) \sin\frac{m\pi x_1}{L_x} \cos\frac{n\pi x_2}{L_y}, \quad (37)$$
$$u_3 = e^{i\omega t} U_3(x_3) \sin\frac{m\pi x_1}{L_x} \sin\frac{n\pi x_2}{L_y}$$

for a simply supported rectangular plate. For $L_x/h = 4$, the first mode corresponds to pure distortional in-plane vibrations of the plate and has null transverse displacements. Modes with zero transverse displacements were missed by Srinivas et al. [14] and other investigators, e.g. [24], who followed the same approach to find, analytically, natural frequencies of a simply supported plate. However, numerical techniques such as the Rayleigh–Ritz method employed by Liew et al. [17] and the FEM used by Batra et al. [21] to solve the 3-dimensional elasticity equations, and the compatible higher order plate theory of Batra and Vidoli [8] in conjunction with the meshless local Petrov–Galerkin method used by

Table 2
Comparison of displacements and transverse stresses computed from the present plate theory with the exact solution of Srinivas et al. [14] for a simply supported rectangular plate; $L_x = L_y$, $L_x/h = \frac{10}{3}$, mode = first antisymmetric ($m = 1$, $n = 1$)

Nondimensional z-coordinate ($2z/h$)	$w(z)/w(0)$			$u(z)/u(0)$		
	Plate theory $K = 5$	Exact	% Error	Plate theory $K = 5$	Exact	% Error
(a) Displacements						
−1	1.0000	1.0000	0	1.0000	1.0000	0
−0.8	1.0249	1.0249	0	0.7561	0.7561	0
−0.6	1.0426	1.0426	0	0.5419	0.5420	0.019
−0.4	1.0543	1.0543	0	0.3495	0.3496	0.029
−0.2	1.0609	1.0610	0.01	0.1712	0.1713	0.058
0	1.0631	1.0631	0	0	0.0000	0
(b) Transverse stresses						
	$\sigma_{33}(z)/\sigma_{33}(-0.2)$			$\sigma_{13}(z)/\sigma_{13}(0)$		
−1	0.0000	0.0000	0	0.0000	0.0000	0.0
−0.8	1.5293	1.5336	0.280	0.3788	0.3750	−1.013
−0.6	1.9841	2.0238	1.962	0.6564	0.6549	−0.229
−0.4	1.7366	1.7578	1.206	0.8486	0.8426	−0.712
−0.2	1.0000	1.0000	0	0.9623	0.9625	0.021
0	0.0000	0.0000	0	1.0000	1.0000	0

Table 3
Comparison of first eight nondimensional frequencies of a clamped rectangular plate ($L_x = 2L_y$) (a) with the solution of Liew and Teo [20] for $L_x/h = 8$ and (b) for $L_x/h = 4$, 12 and 20

Mode	Plate theory $K = 5$	Liew & Teo	% Difference
1(a)	0.5500	0.5422	−1.4455
2(a)	0.6937	0.6787	−2.2045
3(a)	0.9358	0.9020	−3.7542
4(s)	1.0177	1.0144	−0.3273
5(a)	1.1472	1.1259	−1.8873
6(a)	1.2524	1.1826	−5.9058
7(a)	1.2547	1.2316	−1.8765
8(s)	1.3635	1.3575	−0.4405

$L_x/h = 4$		$L_x/h = 12$		$L_x/h = 20$	
Mode	Frequency ($K = 5$)	Mode	Frequency ($K = 3$)	Mode	Frequency ($K = 3$)
1(a)	1.4261	1(a)	0.2844	1(a)	0.1154
2(a)	1.7787	2(a)	0.3616	2(a)	0.1492
3(s)	2.0393	3(a)	0.4957	3(a)	0.2102
4(a)	2.3313	4(a)	0.6383	4(a)	0.2794
5(a)	2.6792	5(a)	0.6760	5(a)	0.2958
6(s)	2.7358	6(s)	0.6774	6(a)	0.3070
7(s)	2.8787	7(a)	0.6983	7(a)	0.3559
8(a)	2.9518	8(a)	0.8014	8(a)	0.4026

Qian et al. [18] predict these frequencies and the in-plane modes of vibration. Batra and Aimmanee [15] have discussed in detail edge conditions and material symmetries which admit these pure distortional modes of vibration. With an increase in the aspect ratio, the frequency of the pure distortional in-plane modes of vibration relative to that of the flexural modes increases. For example, for $L_x/h = 4$, the first, the fourth and the eighth frequencies correspond to pure distortional in-plane modes of vibration but for $L_x/h = 12$, the third and the sixth frequencies are for pure distortional in-plane modes of vibration.

For each value of m and n in (37) there are infinitely many through-the-thickness modes of vibration with frequencies noticeably higher than those of flexural modes, e.g. see Vel and Batra [22]. Batra et al. [13] used the present mixed higher-order shear and normal deformable plate theory to determine natural frequencies and wave propagation in a simply supported orthotropic plate. They assumed the form (37) for displacements and thus simplified the problem considerably. However, expressions (37) for displacements are valid for simply supported plates only.

The non-dimensional frequencey, $\bar{\omega}$, listed in Table 1 is related to the dimensional frequency, ω, by

$$\bar{\omega} = \omega h \sqrt{\frac{2(1+\nu)\rho}{E}}. \tag{38}$$

It is clear that for $L_x/h = 4, 8, 12$ and 20, the computed first ten frequencies match very well with their corresponding analytical values, and the maximum difference between the two is less than 4.2% for $L_x/h = 4$ and 8. A fifth-order mixed shear and normal deformable plate theory was used to compute frequencies of these plates. However, for $L_x/h = 12$ and 20, a third-order mixed shear and normal deformable plate theory was employed, and the error between the computed and the exact first ten frequencies was less than 4.1% for $L_x/h = 12$ and less than 10% for $L_x/h = 20$. The latter rather large difference occurs for the eighth mode that correspond to $m = 5$, $n = 1$. Note that a large value of K captures better the through-the-thickness variation of different field variables. However, to adequately represent variations of displacements in the x_1- and x_2-directions, one needs to refine the FE mesh. The number of nodes used in the x_1-direction is not enough to represent well the four or five half-sine waves in the x_1-direction.

In order to see if the plate theory can accurately predict through-the-thickness distribution of the transverse normal and the transverse shear stresses, we have listed in Table 2 their values computed from the plate theory and the analytical solution. The maximum error in σ_{33} is less than 2% and that in σ_{13} is around 1%; these stresses have been computed from Eqs. $(12)_{4,5}$ of the plate theory.

Table 3 lists first eight natural frequencies for a clamped rectangular plate with $L_x = 2L_y$ and $L_x/h = 4, 8, 12$ and 20. For $L_x/h = 8$, computed frequencies are found to differ from those reported by Liew and Teo [20] by less than 6%; the maximum difference is for the sixth frequency and corresponds to an antisymmetric mode of vibration. Liew and Teo used the differential quadrature method to compute frequencies; thus their solution is also approximate. A comparison of results listed in Tables 1 and 3 reveals that edge conditions significantly influence not only the natural frequency but also the mode shape. As stated by Batra and Aimmanee [15] in-plane pure distortional modes are inadmissible in a clamped plate. With an increase in the aspect ratio from 4 to 20, the first nondimensional natural frequency decreases from 0.7854 to 0.0589 for a simply supported plate and from 1.4261 to 0.1154 for a clamped plate. Whereas for a simply supported plate the mode shape changes from pure distortional for $L_x/h = 4$ to antisymmetric for $L_x/h = 20$, there is no change in the first mode shape for a clamped plate. Fig. 2 exhibits through-the-thickness distributions of the transverse normal stress and the transverse shear stress on two or three vertical lines for the clamped rectangular plate vibrating in the

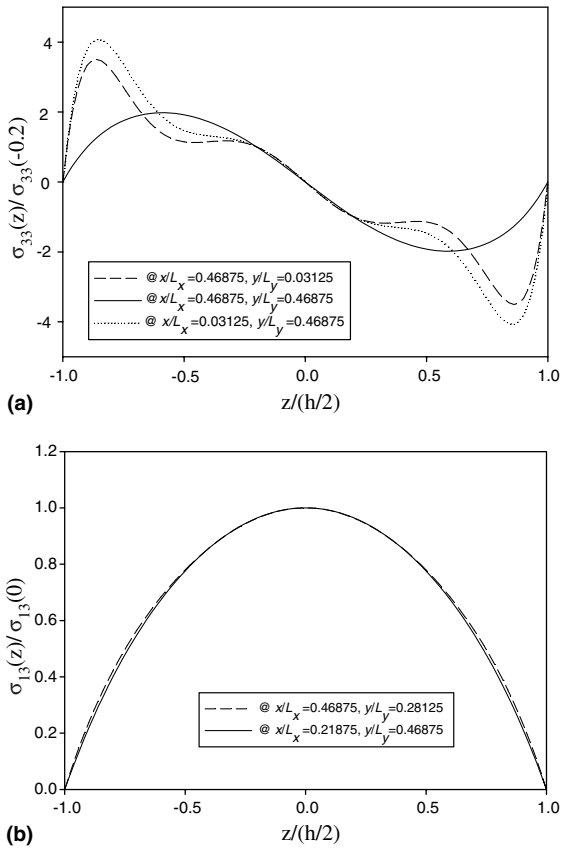

Fig. 2. Through-the-thickness distribution of: (a) the transverse normal stress, and (b) the transverse shear stress for a clamped rectangular plate vibrating in the fundamental mode.

Table 4
First eight nondimensional frequencies of a CFCF rectangular plate ($L_x = 2L_y$) clamped on edges $x_2 = 0$ and $x_2 = L_y$

$L_x/h = 4$		$L_x/h = 8$		$L_x/h = 12$		$L_x/h = 20$	
Mode	Frequency ($K = 5$)	Mode	Frequency ($K = 5$)	Mode	Frequency ($K = 3$)	Mode	Frequency ($K = 3$)
1(a)	1.2974	1(a)	0.5020	1(a)	0.2591	1(a)	0.1048
2(a)	1.3322	2(a)	0.5184	2(a)	0.2688	2(a)	0.1091
3(s)	1.5093	3(a)	0.5902	3(a)	0.3085	3(a)	0.1264
4(a)	1.5196	4(a)	0.7493	4(a)	0.3926	4(a)	0.1630
5(s)	1.9242	5(s)	0.7542	5(s)	0.5018	5(a)	0.2239
6(a)	1.9396	6(s)	0.9630	6(a)	0.5294	6(a)	0.2688
7(a)	2.5350	7(a)	1.0046	7(a)	0.6137	7(a)	0.2740
8(a)	2.5537	8(a)	1.1009	8(a)	0.6251	8(a)	0.2936

fundamental mode. These plots verify that the boundary condition of null tractions on the top and the bottom surfaces are very well satisfied. The through-the-thickness distribution of the transverse shear stress is parabolic and is nearly the same on the two vertical lines considered. Near some points on the clamped surfaces, the transverse normal stress exhibits a boundary-layer like phenomenon.

We have listed in Table 4 the first eight frequencies of a rectangular plate with $L_x = 2L_y$, the edges $x_2 = 0$ and L_y clamped and the other two traction free, and aspect ratio $L_x/h = 4$, 8, 12 and 20. Frequencies of plates with $L_x/h = 4$ and 8 were computed with $K = 5$, and of other plates with $K = 3$. Pure distortional modes are inadmis-

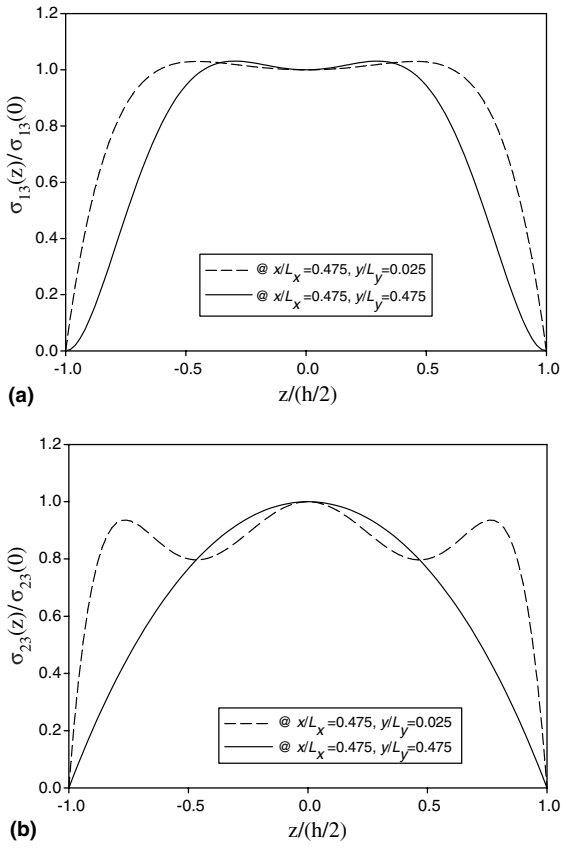

Fig. 3. Through-the-thickness distribution of the transverse shear stress: (a) σ_{13} and (b) σ_{23} for a clamped-free rectangular plate vibrating in the fundamental mode.

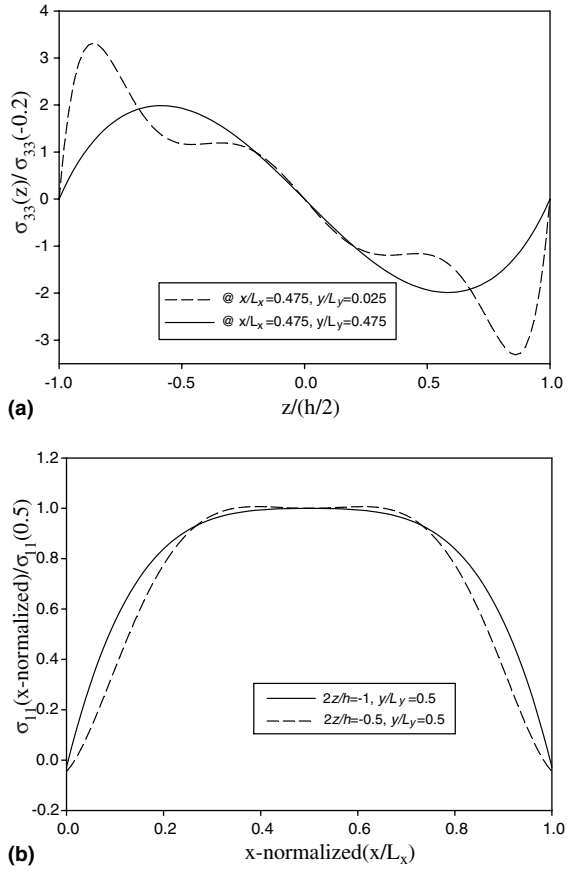

Fig. 4. For a clamped-free rectangular plate vibrating in the first mode: (a) through the thickness distribution of the transverse normal stress on two vertical lines, and (b) the variation of σ_{11} on two horizontal lines.

sible in this plate too. Comparing the first flexural frequency listed in Tables 1, 3 and 4 we find that for each one of the four values of L_x/h, the simply supported plate has the lowest frequency and the clamped plate the highest. For each one of three edge conditions, the first eight frequencies of a plate with $L_x/h = 20$ correspond to antisymmetric modes of vibration but those of a plate with $L_x/h = 4$, 8 and 12 have at least one mode amongst the first eight for which deformations are symmetric about the midsurface of the plate; a plate theory, such as the classical one, that neglects deformations symmetric about the midsurface will not capture this vibration mode. Fig. 3 evinces through-the-thickness distribution of the transverse shear stresses σ_{13} and σ_{23} on two arbitrarily chosen vertical lines. Whereas the variation of σ_{23} is parabolic on one line, on the other line it seems to exhibit a boundary layer type behavior at points adjacent to the top and the bottom traction free surfaces of the plate. The variation of σ_{13} on the two lines is not parabolic. In all of these four cases, σ_{13} and σ_{23} vanish, as they should, on the top and the bottom surfaces of the plate. The through-the-thickness distribution of σ_{33} for a clamped-free plate plotted in Fig. 4a is similar to that of a clamped-clamped plate. Results depicted in Fig. 4b reveal that the axial stress, σ_{11}, is essentially constant in the central (4/10)th of the plate. Again, the boundary condition of $\sigma_{11} = 0$ at $x_1 = 0$ and L_x is well satisfied.

The compatible version of the present mixed higher-order shear and normal deformable plate theory has been successfully used to analyze free and forced vibrations of a thick functionally graded plate [18,25–28].

5. Comparison of present approach with the solution of the 3D problem by the FEM

Batra et al. [21] found that a uniform 40×40 FE mesh of 20-node brick elements with four elements in the thickness direction coupled with three-dimensional linear elasticity equations gives reasonably accurate values of the first ten natural frequencies. Thus displacement components in each direction are approximated with piecewise quadratic functions. This mesh results in 177,147 degrees of freedom (DOF) for a plate free at the edges. With the present plate theory, a 40×40 uniform FE mesh of 8-node elements on the midsurface of the plate and $K = 5$ has 118,098 DOF and gives equally accurate values of first ten natural frequencies, and stress distributions in the plate. Furthermore, in the present plate theory, we can split the free-vibration problem into two sub-problems, i.e., one for symmetric modes and the other for anti-symmetric modes. Thus, the number of DOF in the higher order plate theory for each sub-problem will be 59,049 resulting in a considerable saving in the CPU time relative to that needed for the conventional FEM.

Other differences between the present approach and the FEM are delineated in the following Table 5.

6. Comparison of the present mixed higher order Plate theory with other higher order Plate theories

The key advantages of the present mixed higher order plate theory over other higher order plate theories are listed in Table 6.

Table 5
Comparison of the present approach with the FEM

Item	Present higher-order plate theory	Finite Element method
Input needed	2-dimensional mesh on the mid-surface	3-dimensional mesh
Refine computed frequencies	Increase the order, K, of the plate theory and/or refine the 2-dimensional mesh	Add more elements in the thickness direction and/or in other two directions
Refine through-the-thickness mode shapes	Increase the order, K, of the plate theory	Add more elements in the thickness direction
Through-the-thickness variation of displacements	Polynomial of order K	Usually piecewise linear or quadratic
Variation of displacements in the in-plane directions	Same as for the FEM	
Through-the-thickness variation of transverse stresses	Polynomial of order $(K + 1)$	Usually constant or piecewise linear within each element
Through-the-thickness variation of in-plane stresses	Polynomial of order $(K - 1)$	Usually constant or piecewise linear within each element
Traction boundary conditions on the top and/or the bottom surfaces	Satisfied exactly at every point	Satisfied in the weak sense
Boundary conditions on the edges	Satisfied in the weak sense	Satisfied in the weak sense
Effort required to prepare the input file	Considerably less as compared to that for the FEM	
CPU time	Less as compared to that for the FEM	
Can separate symmetric and antisymmetric modes	Yes	No

Table 6
Comparison of the present mixed higher order plate theory with other higher order plate theories

Item	Present mixed theory	Other theories
Order of polynomial for transverse stresses	$(K+2)$	$(K-1)$
Traction boundary conditions on the top and/or the bottom surfaces	Exactly satisfied	May not be exactly satisfied
Stresses computed from equations of the plate theory	Yes	No
Tangential tractions on the top and/or the bottom surfaces	May be non-zero; exactly satisfied	Tacitly set equal to zero; not exactly satisfied
Equal pressure loads on the top and the bottom surfaces	Make contributions for all values of K	Usually contribute only for $K>0$
Order of governing partial differential equations	2	Generally 4

7. Conclusions

We have used the finite element method and the mixed higher-order shear and normal deformable plate theory of Batra and Vidoli [8] to compute natural frequencies of a rectangular plate made of an isotropic and homogeneous material. The edges of the plate are either simply supported or clamped, or two opposite edges are clamped and the other two are free. The length, L_x, of the plate in the x_1-direction equals either L_y or $2L_y$; L_y being the length in the x_2-direction. The plate theory exactly satisfies boundary conditions of null tractions on the top and the bottom surfaces of the plate. All components of the stress tensor are computed from equations of the plate theory.

For $L_x/h = 4$ and 8, the fifth-order mixed shear and normal deformable plate theory gives frequencies and through-the-thickness distributions of transverse shear and normal stresses that are very close to the analytical solution of the problem for a simply supported plate. For $L_x/h = 12$ and 20, frequencies computed from the third-order plate theory agree well with those obtained from the analytical solution of the problem. First eight frequencies of a clamped rectangular plate with $L_x/L_y = 2$ and $L_x/h = 8$ are found to match well with the results of Liew and Teo [20]. The through-the-thickness distribution of transverse shear stresses suggests the existence of a boundary layer phenomenon adjacent to the top and the bottom surfaces of the plate. Natural frequencies and through-the-thickness distributions of transverse stresses have also been computed for a rectangular plate with two opposite edges clamped and the other two traction free.

Appendix A

For a transversely isotropic material with x_3-axis as the axis of transverse isotropy matrices $\mathbf{C}^{pp}$, $\mathbf{C}^{pt}$, C^{pn}, etc. of Eq. (5) in terms of the more familiar elastic constants are

$$
\begin{aligned}
\mathbf{C}^{pp} &= \frac{1}{E_1}\begin{bmatrix} 1 & -\nu_{12} & 0 \\ -\nu_{12} & 1 & 0 \\ 0 & 0 & 2(1+\nu_{12}) \end{bmatrix}, \\
\mathbf{C}^{pt} &= \begin{bmatrix} 0 & 0 \\ 0 & 0 \\ 0 & 0 \end{bmatrix}, \\
\mathbf{C}^{pn} &= \frac{1}{E_3}\begin{Bmatrix} -\nu_{31} \\ -\nu_{31} \\ 0 \end{Bmatrix}, \\
\mathbf{C}^{tp} &= \begin{bmatrix} 0 & 0 & 0 \\ 0 & 0 & 0 \end{bmatrix}, \\
\mathbf{C}^{tt} &= \begin{bmatrix} 1/\mu_{13} & 0 \\ 0 & 1/\mu_{13} \end{bmatrix}, \\
\mathbf{C}^{tn} &= \begin{Bmatrix} 0 \\ 0 \end{Bmatrix}, \\
\mathbf{C}^{np} &= \left\{ -\tfrac{\nu_{13}}{E_1} \quad -\tfrac{\nu_{13}}{E_1} \quad 0 \right\}, \\
\mathbf{C}^{nt} &= \{ 0 \quad 0 \}, \quad \mathbf{C}^{nn} = \frac{1}{E_3}[1], \quad \frac{\nu_{13}}{E_1} = \frac{\nu_{31}}{E_3}.
\end{aligned}
\tag{39}
$$

In Eqs. (8) E_1 and E_3 are Young's moduli along the x_1- and the x_3-axes, respectively, ν_{12} and ν_{13} are Poisson's ratios in the x_1x_2- and the x_1x_3-planes respectively, and μ_{13} is the shear modulus in the x_1x_3-plane. There are five elastic constants: E_1, E_3, ν_{12}, ν_{13}, μ_{13}.

For an orthotropic material with coordinate planes aligned along the planes of material symmetry

$$
\begin{aligned}
\mathbf{C}^{tp} &= \begin{bmatrix} \frac{1}{E_1} & -\frac{\nu_{12}}{E_1} & 0 \\ -\frac{\nu_{12}}{E_1} & \frac{1}{E_2} & 0 \\ 0 & 0 & \frac{1}{\mu_{12}} \end{bmatrix}, \\
\mathbf{C}^{pt} &= \begin{bmatrix} 0 & 0 \\ 0 & 0 \\ 0 & 0 \end{bmatrix}, \quad \mathbf{C}^{pn} = \begin{Bmatrix} -\nu_{13}/E_1 \\ -\nu_{23}/E_2 \\ 0 \end{Bmatrix}, \\
\mathbf{C}^{tp} &= \begin{bmatrix} 0 & 0 & 0 \\ 0 & 0 & 0 \end{bmatrix}, \\
\mathbf{C}^{tt} &= \begin{bmatrix} \frac{1}{\mu_{13}} & 0 \\ 0 & \frac{1}{\mu_{23}} \end{bmatrix},
\end{aligned}
$$

$$\mathbf{C}^{tn} = \begin{Bmatrix} 0 \\ 0 \end{Bmatrix},$$
$$\mathbf{C}^{np} = \begin{bmatrix} -\frac{\nu_{31}}{E_3} & -\frac{\nu_{32}}{E_3} & 0 \end{bmatrix}, \quad \mathbf{C}^{nt} = [0 \quad 0],$$
$$\mathbf{C}^{nn} = \frac{1}{E_3}[1], \quad \frac{\nu_{13}}{E_1} = \frac{\nu_{31}}{E_3}, \quad \frac{\nu_{23}}{E_2} = \frac{\nu_{32}}{E_3}. \tag{40}$$

Here E_1, E_2 and E_3 are Young's moduli along the x_1-, x_2- and x_3-axes respectively, ν_{12}, ν_{23} and ν_{13} are Poisson's ratios and μ_{12}, μ_{23} and μ_{13} are shear moduli in the x_1x_2-, x_2x_3- and x_3x_1- planes respectively. Nine elastic constants characterize an orthotropic material.

For monoclinic, triclinic, hexagonal and trigonal materials, it is simpler to use numerical values of elastic constants to find the compliances.

Appendix B

For $K = 7$, modified Legendre polynomials are

$$\widetilde{L}_0(z) = \frac{\sqrt{2}}{256}(93 + 1260z^2 - 6930z^4 + 12012z^6 - 6435z^8),$$
$$\widetilde{L}_1(z) = \frac{1}{256}\sqrt{\frac{2}{3}}(-561z + 13860z^3 - 54054z^5 + 7320z^7 - 36465z^9),$$
$$\widetilde{L}_2(z) = \frac{1}{256}\sqrt{\frac{2}{5}}(-495 + 7260z^2 - 34650z^4 + 60060z^6 - 32175z^8),$$
$$\widetilde{L}_3(z) = \frac{1}{256}\sqrt{\frac{2}{7}}(-3549z + 34580z^3 - 126126z^5 + 180180z^7 - 85085z^9),$$
$$\widetilde{L}_4(z) = \frac{1}{256}\frac{\sqrt{2}}{3}(117 + 7020z^2 - 57330z^4 + 108108z^6 - 57915z^8),$$
$$\widetilde{L}_5(z) = \frac{1}{256}\sqrt{\frac{2}{11}}(-825z + 27300z^3 - 187110z^5 + 283140z^7 - 133705z^9),$$
$$\widetilde{L}_6(z) = \frac{1}{256}\sqrt{\frac{2}{13}}(-975 + 27300z^2 - 122850z^4 + 180180z^6 - 83665z^8),$$
$$\widetilde{L}_7(z) = \frac{1}{256}\sqrt{\frac{2}{15}}(-8925z + 107100z^3 - 353430z^5 + 437580z^7 - 182325z^9).$$

Appendix C

For $K = 5$, balance equations (17) for a plate with null body forces become the following 18 equations:

$$N^{(0)}_{\alpha\beta,\beta} = \rho\ddot{u}^{(0)}_\alpha, \ \alpha = 1,2,$$
$$N^{(1)}_{\alpha\beta,\beta} - \sqrt{3}T^{(0)}_\alpha = \rho\ddot{u}^{(1)}_\alpha,$$
$$N^{(2)}_{\alpha\beta,\beta} - \sqrt{15}T^{(1)}_\alpha = \rho\ddot{u}^{(2)}_\alpha,$$
$$N^{(3)}_{\alpha\beta,\beta} - \sqrt{7}T^{(0)}_\alpha - \sqrt{35}T^{(2)}_\alpha = \rho\ddot{u}^{(3)}_\alpha,$$
$$N^{(4)}_{\alpha\beta,\beta} - 3\sqrt{3}T^{(1)}_\alpha - 3\sqrt{7}T^{(3)}_\alpha = \rho\ddot{u}^{(4)}_\alpha,$$
$$N^{(5)}_{\alpha\beta,\beta} - \sqrt{11}T^{(0)}_\alpha - \sqrt{55}T^{(2)}_\alpha - 3\sqrt{13}T^{(4)}_\alpha = \rho\ddot{u}^{(5)}_\alpha;$$

$$T^{(0)}_{\alpha,\alpha} = \rho\ddot{u}^{(0)}_3,$$
$$T^{(1)}_{\alpha,\alpha} - \sqrt{3}\Sigma^{(0)} = \rho\ddot{u}^{(1)}_3,$$
$$T^{(2)}_{\alpha,\alpha} - \sqrt{15}\Sigma^{(1)} = \rho\ddot{u}^{(2)}_3,$$
$$T^{(3)}_{\alpha,\alpha} - \sqrt{7}\Sigma^{(0)} - \sqrt{35}\Sigma^{(2)} = \rho\ddot{u}^{(3)}_3,$$
$$T^{(4)}_{\alpha,\alpha} - 3\sqrt{3}\Sigma^{(1)} - 3\sqrt{7}\Sigma^{(3)} = \rho\ddot{u}^{(4)}_3,$$
$$T^{(5)}_{\alpha,\alpha} - \sqrt{11}\Sigma^{(0)} - \sqrt{55}\Sigma^{(2)} - 3\sqrt{13}\Sigma^{(4)} = \rho\ddot{u}^{(5)}_3.$$

For a free plate (i.e. null tractions on its top and bottom surfaces) made of an isotropic material, and $K = 1$, 3 and 5, the solution of equations (18) for $\mathbf{N}^{(a)}$, $\mathbf{T}^{(a)}$ and $\Sigma^{(a)}$ in terms of strains is given below.

$K = 1$

$$N^{(0)}_{11} = \left(\frac{E(5\nu^2 - 6)\hat{e}^{(0)}_{11}}{2(5\nu^3 + 8\nu^2 - 3)} - \frac{E\nu(5\nu + 6)\hat{e}^{(0)}_{22}}{2(5\nu^3 + 8\nu^2 - 3)} - \frac{5E\nu(\nu + 1)\epsilon^{(0)}}{2(5\nu^3 + 8\nu^2 - 3)}\right),$$
$$N^{(1)}_{11} = \left(\frac{E(7\nu^2 - 10)\hat{e}^{(1)}_{11}}{2(7\nu^3 + 12\nu^2 - 5)} - \frac{E\nu(7\nu + 10)\hat{e}^{(1)}_{22}}{2(7\nu^3 + 12\nu^2 - 5)} - \frac{7E\nu(\nu + 1)\epsilon^{(1)}}{2(7\nu^3 + 12\nu^2 - 5)}\right),$$
$$N^{(0)}_{12} = \frac{E\hat{e}^{(0)}_{12}}{\nu + 1},$$
$$N^{(1)}_{12} = \frac{E\hat{e}^{(1)}_{12}}{\nu + 1},$$
$$N^{(0)}_{22} = \left(-\frac{E(5\nu^2 + 6\nu)\hat{e}^{(0)}_{11}}{2(5\nu^3 + 8\nu^2 - 3)} - \frac{E(6 - 5\nu^2)\hat{e}^{(0)}_{22}}{2(5\nu^3 + 8\nu^2 - 3)} - \frac{E(5\nu^2 + 5\nu)\epsilon^{(0)}}{2(5\nu^3 + 8\nu^2 - 3)}\right),$$
$$N^{(1)}_{22} = \left(-\frac{E(7\nu^2 + 10\nu)\hat{e}^{(1)}_{11}}{2(7\nu^3 + 12\nu^2 - 5)} - \frac{E(10 - 7\nu^2)\hat{e}^{(1)}_{22}}{2(7\nu^3 + 12\nu^2 - 5)} - \frac{E(7\nu^2 + 7\nu)\epsilon^{(1)}}{2(7\nu^3 + 12\nu^2 - 5)}\right),$$
$$T^{(0)}_1 = \frac{5E\gamma^{(0)}_1}{6(\nu + 1)},$$

$$T_1^{(1)} = \frac{7E\gamma_1^{(1)}}{10(v+1)},$$

$$T_2^{(0)} = \frac{5E\gamma_2^{(0)}}{6(v+1)},$$

$$T_2^{(1)} = \frac{7E\gamma_2^{(1)}}{10(v+1)},$$

$$\Sigma^{(0)} = \left(-\frac{5Ev\hat{e}_{11}^{(0)}}{10v^2+6v-6} - \frac{5Ev\hat{e}_{22}^{(0)}}{10v^2+6v-6} - \frac{5E(1-v)\gamma^{(0)}}{10v^2+6v-6} \right),$$

$$\Sigma^{(1)} = \left(-\frac{7Ev\hat{e}_{11}^{(1)}}{2(7v^2+5v-5)} - \frac{7Ev\hat{e}_{22}^{(1)}}{2(7v^2+5v-5)} - \frac{7E(1-v)\epsilon^{(1)}}{2(7v^2+5v-5)} \right).$$

$K = 3$

$$N_{11}^{(0)} = \left(-\frac{\sqrt{5}E\hat{e}_{11}^{(2)}}{3(v+1)(12v^3+4v^2-15v+5)} \times \frac{\sqrt{5}E\hat{e}_{22}^{(2)}}{3(v+1)(12v^3+4v^2-15v+5)} + \frac{E(18v^3-4v^2-30v+15)\hat{e}_{11}^{(0)}}{3(v+1)(12v^3+4v^2-15v+5)} + \frac{E(-18v^3-16v^2+15v)\hat{e}_{22}^{(0)}}{3(v+1)(12v^3+4v^2-15v+5)} + \frac{E(-18v^3-14v^2+14v)\epsilon^{(0)}}{3(v+1)(12v^3+4v^2-15v+5)} + \frac{E(\sqrt{5}v^2-\sqrt{5}v)\epsilon^{(2)}}{3(v+1)(12v^3+4v^2-15v+5)} \right),$$

$$N_{11}^{(1)} = \left(-\frac{\sqrt{21}E\hat{e}_{11}^{(3)}v^2}{(v+1)(44v^3+20v^2-63v+21)} - \frac{\sqrt{21}E\hat{e}_{22}^{(3)}v^2}{(v+1)(44v^3+20v^2-63v+21)} + \frac{E(22v^3-4v^2-42v+21)\hat{e}_{11}^{(1)}}{(v+1)(44v^3+20v^2-63v+21)} + \frac{E(-22v^3-24v^2+21v)\hat{e}_{22}^{(1)}}{(v+1)(44v^3+20v^2-63v+21)} + \frac{E(-22v^3-18v^2+18v)\epsilon^{(1)}}{(v+1)(44v^3+20v^2-63v+21)} + \frac{E(\sqrt{21}v^2-\sqrt{21}v)\epsilon^{(3)}}{(v+1)(44v^3+20v^2-63v+21)} \right),$$

$$N_{11}^{(1)} = \left(-\frac{\sqrt{5}E\hat{e}_{11}^{(0)}v^2}{3(v+1)(12v^3+4v^2-15v+5)} - \frac{\sqrt{5}E\hat{e}_{22}^{(0)}v^2}{3(v+1)(12v^3+4v^2-15v+5)} - \frac{E(-18v^3+8v^2+30v-15)\hat{e}_{11}^{(2)}}{3(v+1)(12v^3+4v^2-15v+5)} - \frac{E(18v^3+20v^2-15v)\hat{e}_{22}^{(2)}}{3(v+1)(12v^3+4v^2-15v+5)} - \frac{E(\sqrt{5}v-\sqrt{5}v^2)\epsilon^{(0)}}{3(v+1)(12v^3+4v^2-15v+5)} - \frac{E(18v^3+10v^2-10v)\epsilon^{(2)}}{3(v+1)(12v^3+4v^2-15v+5)} \right),$$

$$N_{11}^{(3)} = \left(-\frac{\sqrt{21}E\hat{e}_{11}^{(1)}v^2}{(v+1)(44v^3+20v^2-63v+21)} - \frac{\sqrt{21}E\hat{e}_{22}^{(1)}v^2}{(v+1)(44v^3+20v^2-63v+21)} - \frac{E(-22v^3+8v^2+42v-21)\hat{e}_{11}^{(3)}}{(v+1)(44v^3+20v^2-63v+21)} - \frac{E(22v^3+28v^2-21v)\hat{e}_{22}^{(3)}}{(v+1)(44v^3+20v^2-63v+21)} - \frac{E(\sqrt{21}v-\sqrt{21}v^2)\epsilon^{(1)}}{(v+1)(44v^3+20v^2-63v+21)} - \frac{E(22v^3+14v^2-14v)\epsilon^{(3)}}{(v+1)(44v^3+20v^2-63v+21)} \right),$$

$$N_{12}^{(0)} = \frac{E\hat{e}_{12}^{(0)}}{v+1},$$

$$N_{12}^{(1)} = \frac{E\hat{e}_{12}^{(1)}}{v+1},$$

$$N_{12}^{(2)} = \frac{E\hat{e}_{12}^{(2)}}{v+1},$$

$$N_{12}^{(3)} = \frac{E\hat{e}_{12}^{(3)}}{v+1},$$

$$N_{22}^{(0)} = \left(-\frac{\sqrt{5}E\hat{e}_{11}^{(2)}v^2}{3(v+1)(12v^3+4v^2-15v+5)} - \frac{\sqrt{5}E\hat{e}_{22}^{(2)}v^2}{3(v+1)(12v^3+4v^2-15v+5)} - \frac{E(18v^3+16v^2-15v)\hat{e}_{11}^{(0)}}{3(v+1)(12v^3+4v^2-15v+5)} - \frac{E(-18v^3+4v^2+30v-15)\hat{e}_{22}^{(0)}}{3(v+1)(12v^3+4v^2-15v+5)} - \frac{E(18v^3+14v^2-14v)\epsilon^{(0)}}{3(v+1)(12v^3+4v^2-15v+5)} - \frac{E(\sqrt{5}v-\sqrt{5}v^2)\epsilon^{(2)}}{3(v+1)(12v^3+4v^2-15v+5)} \right),$$

$$N_{22}^{(1)} = \left(-\frac{\sqrt{21}E\hat{e}_{11}^{(3)}v^2}{(v+1)(44v^3+20v^2-63v+21)} - \frac{\sqrt{21}E\hat{e}_{22}^{(3)}v^2}{(v+1)(44v^3+20v^2-63v+21)} - \frac{E(22v^3+24v^2-21v)\hat{e}_{11}^{(1)}}{(v+1)(44v^3+20v^2-63v+21)} - \frac{E(-22v^3+4v^2+42v-21)\hat{e}_{22}^{(1)}}{(v+1)(44v^3+20v^2-63v+21)} - \frac{E(22v^3+18v^2-18v)\epsilon^{(1)}}{(v+1)(44v^3+20v^2-63v+21)} - \frac{E(\sqrt{21}v-\sqrt{21}v^2)\epsilon^{(3)}}{(v+1)(44v^3+20v^2-63v+21)} \right),$$

$$N_{22}^{(2)} = \left(-\frac{\sqrt{5}E\hat{e}_{11}^{(0)}v^2}{3(v+1)(12v^3+4v^2-15v+5)} - \frac{\sqrt{5}E\hat{e}_{22}^{(0)}v^2}{3(v+1)(12v^3+4v^2-15v+5)} - \frac{E(18v^3+20v^2-15v)\hat{e}_{11}^{(2)}}{3(v+1)(12v^3+4v^2-15v+5)} - \frac{E(-18v^3+8v^2+30v-15)\hat{e}_{22}^{(2)}}{3(v+1)(12v^3+4v^2-15v+5)} - \frac{E(\sqrt{5}v-\sqrt{5}v^2)\epsilon^{(0)}}{3(v+1)(12v^3+4v^2-15v+5)} - \frac{E(18v^3+10v^2-10v)\epsilon^{(2)}}{3(v+1)(12v^3+4v^2-15v+5)} \right),$$

$$N_{22}^{(3)} = \left(-\frac{\sqrt{21}E\hat{e}_{11}^{(1)}v^2}{(v+1)(44v^3+20v^2-63v+21)} - \frac{\sqrt{21}E\hat{e}_{22}^{(1)}v^2}{(v+1)(44v^3+20v^2-63v+21)} - \frac{E(22v^3+28v^2-21v)\hat{e}_{11}^{(3)}}{(v+1)(44v^3+20v^2-63v+21)} - \frac{E(-22v^3+8v^2+42v-21)\hat{e}_{22}^{(3)}}{(v+1)(44v^3+20v^2-63v+21)} - \frac{E(\sqrt{21}v-\sqrt{21}v^2)\epsilon^{(1)}}{(v+1)(44v^3+20v^2-63v+21)} - \frac{E(22v^3+14v^2-14v)\epsilon^{(3)}}{(v+1)(44v^3+20v^2-63v+21)} \right),$$

$$T_1^{(0)} = \left(\frac{14E\gamma_1^{(0)}}{15(v+1)} - \frac{E\gamma_1^{(2)}}{3\sqrt{5}(v+1)} \right),$$

$$T_1^{(1)} = \left(\frac{6E\gamma_1^{(1)}}{7(v+1)} - \frac{E\gamma_1^{(3)}}{\sqrt{21}(v+1)} \right),$$

$$T_1^{(2)} = \left(\frac{2E\gamma_1^{(2)}}{3(v+1)} - \frac{E\gamma_1^{(0)}}{3\sqrt{5}(v+1)} \right),$$

$$T_1^{(3)} = \left(\frac{2E\gamma_1^{(3)}}{3(v+1)} - \frac{E\gamma_1^{(1)}}{\sqrt{21}(v+1)} \right),$$

$$T_2^{(0)} = \left(\frac{14E\gamma_2^{(0)}}{15(v+1)} - \frac{E\gamma_2^{(2)}}{3\sqrt{5}(v+1)} \right),$$

$$T_2^{(1)} = \left(\frac{6E\gamma_2^{(1)}}{7(v+1)} - \frac{E\gamma_2^{(3)}}{\sqrt{21}(v+1)} \right),$$

$$T_2^{(2)} = \left(\frac{2E\gamma_2^{(2)}}{3(v+1)} - \frac{E\gamma_2^{(0)}}{3\sqrt{5}(v+1)} \right),$$

$$T_2^{(3)} = \left(\frac{2E\gamma_2^{(3)}}{3(v+1)} - \frac{E\gamma_2^{(1)}}{\sqrt{21}(v+1)} \right),$$

$$\Sigma^{(0)} = \left(-\frac{E(18v^3+14v^2-14v)\hat{e}_{11}^{(0)}}{3(v+1)(12v^3+4v^2-15v+5)} - \frac{E(\sqrt{5}v-\sqrt{5}v^2)\hat{e}_{11}^{(2)}}{3(v+1)(12v^3+4v^2-15v+5)} - \frac{E(18v^3+14v^2-14v)\hat{e}_{22}^{(0)}}{3(v+1)(12v^3+4v^2-15v+5)} - \frac{E(\sqrt{5}v-\sqrt{5}v^2)\hat{e}_{22}^{(2)}}{3(v+1)(12v^3+4v^2-15v+5)} - \frac{E(-18v^3+4v^2+28v-14)\epsilon^{(0)}}{3(v+1)(12v^3+4v^2-15v+5)} - \frac{E(\sqrt{5}v^2-2\sqrt{5}v+\sqrt{5})\epsilon^{(2)}}{3(v+1)(12v^3+4v^2-15v+5)} \right),$$

$$\Sigma^{(1)} = \left(-\frac{E(22v^3+18v^2-18v)\hat{e}_{11}^{(1)}}{(v+1)(44v^3+20v^2-63v+21)} - \frac{E(\sqrt{21}v-\sqrt{21}v^2)\hat{e}^{(3)}22}{(v+1)(44v^3+20v^2-63v+21)} - \frac{E(22v^3+18v^2-18v)\hat{e}_{22}^{(1)}}{(v+1)(44v^3+20v^2-63v+21)} - \frac{E(\sqrt{21}v-\sqrt{21}v^2)\hat{e}_{22}^{(3)}}{(v+1)(44v^3+20v^2-63v+21)} - \frac{E(-22v^3+4v^2+36v-18)\epsilon^{(1)}}{(v+1)(44v^3+20v^2-63v+21)} - \frac{E(\sqrt{21}v^2-2\sqrt{21}v+\sqrt{21})\epsilon^{(3)}}{(v+1)(44v^3+20v^2-63v+21)} \right),$$

$$\Sigma^{(2)} = \left(-\frac{E(\sqrt{5}v - \sqrt{5}v^2)\hat{e}_{11}^{(0)}}{3(v+1)(12v^3+4v^2-15v+5)} - \frac{E(18v^3+10v^2-10v)\hat{e}_{11}^{(2)}}{3(v+1)(12v^3+4v^2-15v+5)} - \frac{E(\sqrt{5}v - \sqrt{5}v^2)\hat{e}_{22}^{(0)}}{3(v+1)(12v^3+4v^2-15v+5)} - \frac{E(18v^3+10v^2-10v)\hat{e}_{22}^{(2)}}{3(v+1)(12v^3+4v^2-15v+5)} - \frac{E(\sqrt{5}v^2 - 2\sqrt{5}v + \sqrt{5})\epsilon^{(0)}}{3(v+1)(12v^3+4v^2-15v+5)} - \frac{E(-18v^3+8v^2+20v-10)\epsilon^{(2)}}{3(v+1)(12v^3+4v^2-15v+5)} \right),$$

$$\Sigma^{(3)} = \left(-\frac{E(\sqrt{21}v - \sqrt{21}v^2)\hat{e}_{11}^{(1)}}{(v+1)(44v^3+20v^2-63v+21)} - \frac{E(22v^3+14v^2-14v)\hat{e}_{11}^{(3)}}{(v+1)(44v^3+20v^2-63v+21)} - \frac{E(\sqrt{21}v - \sqrt{21}v^2)\hat{e}_{22}^{(1)}}{(v+1)(44v^3+20v^2-63v+21)} - \frac{E(22v^3+14v^2-14v)\hat{e}_{22}^{(3)}}{(v+1)(44v^3+20v^2-63v+21)} - \frac{E(\sqrt{21}v^2 - 2\sqrt{21}v + \sqrt{21})\epsilon^{(1)}}{(v+1)(44v^3+20v^2-63v+21)} - \frac{E(-22v^3+8v^2+28v-14)\epsilon^{(3)}}{(v+1)(44v^3+20v^2-63v+21)} \right).$$

$K = 5$

$$N_{11}^{(0)} = E\left(-\frac{\sqrt{5}\hat{e}_{11}^{(2)}v^2}{2(v+1)(2v-1)(13v^2+14v-14)} - \frac{3\hat{e}_{11}^{(4)}v^2}{2(v+1)(2v-1)(13v^2+14v-14)} - \frac{\sqrt{5}\hat{e}_{22}^{(2)}v^2}{2(v+1)(2v-1)(13v^2+14v-14)} - \frac{3\hat{e}_{22}^{(4)}v^2}{2(v+1)(2v-1)(13v^2+14v-14)} + \frac{(26v^3+v^2-56v+28)\hat{e}_{11}^{(0)}}{2(v+1)(2v-1)(13v^2+14v-14)} + \frac{(-26v^3-29v^2+28v)\hat{e}_{22}^{(0)}}{2(v+1)(2v-1)(13v^2+14v-14)} + \frac{(-26v^3-27v^2+27v)\hat{e}_{33}^{(0)}}{2(v+1)(2v-1)(13v^2+14v-14)} + \frac{(\sqrt{5}v^2 - \sqrt{5}v)\hat{e}_{33}^{(2)}}{2(v+1)(2v-1)(13v^2+14v-14)} + \frac{(3v^2-3v)\hat{e}_{33}^{(4)}}{2(v+1)(2v-1)(13v^2+14v-14)} \right),$$

$$N_{11}^{(1)} = E\left(-\frac{\sqrt{\frac{7}{3}}\hat{e}_{11}^{(3)}v^2}{2(v+1)(2v-1)(5v^2+6v-6)} - \frac{\sqrt{\frac{11}{3}}\hat{e}_{11}^{(5)}v^2}{2(v+1)(2v-1)(5v^2+6v-6)} - \frac{\sqrt{\frac{7}{3}}\hat{e}_{22}^{(3)}v^2}{2(v+1)(2v-1)(5v^2+6v-6)} - \frac{\sqrt{\frac{11}{3}}\hat{e}_{22}^{(5)}v^2}{2(v+1)(2v-1)(5v^2+6v-6)} + \frac{(10v^3+v^2-24v+12)\hat{e}_{11}^{(1)}}{2(v+1)(2v-1)(5v^2+6v-6)} + \frac{(-30v^3-39v^2+36v)\hat{e}_{22}^{(1)}}{6(v+1)(2v-1)(5v^2+6v-6)} + \frac{(-30v^3-33v^2+33v)\epsilon^{(1)}}{6(v+1)(2v-1)(5v^2+6v-6)} + \frac{(\sqrt{21}v^2 - \sqrt{21}v)\epsilon^{(3)}}{6(v+1)(2v-1)(5v^2+6v-6)} + \frac{(\sqrt{33}v^2 - \sqrt{33}v)\epsilon^{(5)}}{6(v+1)(2v-1)(5v^2+6v-6)} \right),$$

$$N_{11}^{(2)} = E\left(-\frac{\sqrt{5}\hat{e}_{11}^{(0)}v^2}{2(v+1)(2v-1)(13v^2+14v-14)} - \frac{3\sqrt{5}\hat{e}_{11}^{(4)}v^2}{2(v+1)(2v-1)(13v^2+14v-14)} - \frac{\sqrt{5}\hat{e}_{22}^{(0)}v^2}{2(v+1)(2v-1)(13v^2+14v-14)} - \frac{3\sqrt{5}\hat{e}_{22}^{(4)}v^2}{2(v+1)(2v-1)(13v^2+14v-14)} - \frac{(-26v^3+3v^2+56v-28)\hat{e}_{11}^{(2)}}{2(v+1)(2v-1)(13v^2+14v-14)} - \frac{(26v^3+33v^2-28v)\hat{e}_{22}^{(2)}}{2(v+1)(2v-1)(13v^2+14v-14)} - \frac{(\sqrt{5}v - \sqrt{5}v^2)\epsilon^{(0)}}{2(v+1)(2v-1)(13v^2+14v-14)} - \frac{(26v^3+23v^2-23v)\epsilon^{(2)}}{2(v+1)(2v-1)(13v^2+14v-14)} - \frac{(3\sqrt{5}v - 3\sqrt{5}v^2)\epsilon^{(4)}}{2(v+1)(2v-1)(13v^2+14v-14)} \right),$$

$$N_{11}^{(3)} = E\left(-\frac{\sqrt{\frac{7}{3}}\hat{e}_{11}^{(1)}v^2}{2(v+1)(2v-1)(5v^2+6v-6)} - \frac{\sqrt{77}\hat{e}_{11}^{(5)}v^2}{6(v+1)(2v-1)(5v^2+6v-6)} \right.$$

$$
\begin{aligned}
&-\frac{\sqrt{\frac{7}{3}}\hat{e}_{22}^{(1)}v^2}{2(v+1)(2v-1)(5v^2+6v-6)}\\
&-\frac{\sqrt{77}\hat{e}_{22}^{(5)}v^2}{6(v+1)(2v-1)(5v^2+6v-6)}\\
&-\frac{(-30v^3+v^2+72v-36)\hat{e}_{11}^{(3)}}{6(v+1)(2v-1)(5v^2+6v-6)}\\
&-\frac{(30v^3+43v^2-36v)\hat{e}_{22}^{(3)}}{6(v+1)(2v-1)(5v^2+6v-6)}\\
&-\frac{(\sqrt{21}v-\sqrt{21}v^2)\epsilon^{(1)}}{6(v+1)(2v-1)(5v^2+6v-6)}\\
&-\frac{(30v^3+29v^2-29v)\epsilon^{(3)}}{6(v+1)(2v-1)(5v^2+6v-6)}\\
&-\frac{(\sqrt{77}v-\sqrt{77}v^2)\epsilon^{(5)}}{6(v+1)(2v-1)(5v^2+6v-6)}\Bigg),
\end{aligned}
$$

$$
\begin{aligned}
N_{11}^{(4)} = E\Bigg(&-\frac{3\hat{e}_{11}^{(0)}v^2}{2(v+1)(2v-1)(13v^2+14v-14)}\\
&-\frac{3\sqrt{5}\hat{e}_{11}^{(2)}v^2}{2(v+1)(2v-1)(13v^2+14v-14)}\\
&-\frac{3\hat{e}_{22}^{(0)}v^2}{2(v+1)(2v-1)(13v^2+14v-14)}\\
&-\frac{3\sqrt{5}\hat{e}_{22}^{(2)}v^2}{2(v+1)(2v-1)(13v^2+14v-14)}\\
&+\frac{(26v^3-7v^2-56v+28)\hat{e}_{11}^{(4)}}{2(v+1)(2v-1)(13v^2+14v-14)}\\
&+\frac{(-26v^3-37v^2+28v)\hat{e}_{22}^{(2)}}{2(v+1)(2v-1)(13v^2+14v-14)}\\
&+\frac{(3v^2-3v)\epsilon^{(0)}}{2(v+1)(23v-1)(13v^2+14v-14)}\\
&+\frac{(3\sqrt{5}v^2-3\sqrt{5}v)\epsilon^{(2)}}{2(v+1)(2v-1)(13v^2+14v-14)}\\
&+\frac{(-26v^3-19v^2+19v)\epsilon^{(4)}}{2(v+1)(2v-1)(13v^2+14v-14)}\Bigg),
\end{aligned}
$$

$$
\begin{aligned}
N_{11}^{(5)} = E\Bigg(&-\frac{\sqrt{\frac{11}{3}}\hat{e}_{11}^{(1)}v^2}{2(v+1)(2v-1)(5v^2+6v-6)}\\
&-\frac{\sqrt{77}\hat{e}_{11}^{(3)}v^2}{6(v+1)(2v-1)(5v^2+6v-6)}\\
&-\frac{\sqrt{\frac{11}{3}}\hat{e}_{22}^{(1)}v^2}{2(v+1)(2v-1)(5v^2+6v-6)}\\
&-\frac{\sqrt{77}\hat{e}_{22}^{(3)}v^2}{6(v+1)(2v-1)(5v^2+6v-6)}\\
&-\frac{(-30v^3+5v^2+72v-36)\hat{e}_{11}^{(5)}}{6(v+1)(2v-1)(5v^2+6v-6)}\\
&-\frac{(30v^3+47v^2-36v)\hat{e}_{22}^{(5)}}{6(v+1)(2v-1)(5v^2+6v-6)}\\
&-\frac{(\sqrt{33}v-\sqrt{33}v^2)\epsilon^{(1)}}{6(v+1)(2v-1)(5v^2+6v-6)}\\
&-\frac{(\sqrt{77}v-\sqrt{77})v^2\epsilon^{(3)}}{6(v+1)(2v-1)(5v^2+6v-6)}\\
&-\frac{(30v^3+25v^2-25v)\epsilon^{(5)}}{6(v+1)(2v-1)(5v^2+6v-6)}\Bigg),
\end{aligned}
$$

$$
\begin{aligned}
N_{12}^{(0)} &= \frac{E\hat{e}_{12}^{(0)}}{v+1},\\
N_{12}^{(1)} &= \frac{E\hat{e}_{12}^{(1)}}{v+1},\\
N_{12}^{(2)} &= \frac{E\hat{e}_{12}^{(2)}}{v+1},\\
N_{12}^{(3)} &= \frac{E\hat{e}_{12}^{(3)}}{v+1},\\
N_{12}^{(4)} &= \frac{E\hat{e}_{12}^{(4)}}{v+1},\\
N_{12}^{(5)} &= \frac{E\hat{e}_{12}^{(5)}}{v+1},
\end{aligned}
$$

$$
\begin{aligned}
N_{22}^{(0)} = E\Bigg(&-\frac{\sqrt{5}\hat{e}_{11}^{(2)}v^2}{2(v+1)(2v-1)(13v^2+14v-14)}\\
&-\frac{3\hat{e}_{11}^{(4)}v^2}{2(v+1)(2v-1)(13v^2+14v-14)}\\
&-\frac{\sqrt{5}\hat{e}_{22}^{(2)}v^2}{2(v+1)(2v-1)(13v^2+14v-14)}\\
&-\frac{3\hat{e}_{22}^{(4)}v^2}{2(v+1)(2v-1)(13v^2+14v-14)}\\
&-\frac{(26v^3+29v^2-28v)\hat{e}_{11}^{(0)}}{2(v+1)(2v-1)(13v^2+14v-14)}\\
&-\frac{(-26v^3-v^2+56v-28)\hat{e}_{22}^{(0)}}{2(v+1)(2v-1)(13v^2+14v-14)}\\
&-\frac{(26v^3+27v^2-27v)\epsilon^{(0)}}{2(v+1)(2v-1)(13v^2+14v-14)}\\
&-\frac{(\sqrt{5}v-\sqrt{5}v^2)\epsilon^{(2)}}{2(v+1)(2v-1)(13v^2+14v-14)}\\
&-\frac{(3v-3v^2)\epsilon^{(4)}}{2(v+1)(2v-1)(13v^2+14v-14)}\Bigg),
\end{aligned}
$$

$$
\begin{aligned}
N_{22}^{(1)} = E\Bigg(&-\frac{\sqrt{\frac{7}{3}}\hat{e}_{11}^{(3)}v^2}{2(v+1)(2v-1)(5v^2+6v-6)}\\
&-\frac{\sqrt{\frac{11}{3}}\hat{e}_{11}^{(5)}v^2}{2(v+1)(2v-1)(5v^2+6v-6)}
\end{aligned}
$$

$$
\begin{aligned}
&-\frac{\sqrt{\frac{7}{3}}\hat{e}_{22}^{(3)}v^2}{2(v+1)(2v-1)(5v^2+6v-6)}\\
&-\frac{\sqrt{\frac{11}{3}}\hat{e}_{22}^{(5)}v^2}{2(v+1)(2v-1)(5v^2+6v-6)}\\
&-\frac{(30v^3+39v^2-36v)\hat{e}_{11}^{(1)}}{6(v+1)(2v-1)(5v^2+6v-6)}\\
&-\frac{(-30v^3-3v^2+72v-36)\hat{e}_{22}^{(1)}}{6(v+1)(2v-1)(5v^2+6v-6)}\\
&-\frac{(30v^3+33v^2-33v)\epsilon^{(1)}}{6(v+1)(2v-1)(5v^2+6v-6)}\\
&-\frac{(\sqrt{21}v-\sqrt{21}v^2)\epsilon^{(3)}}{6(v+1)(2v-1)(5v^2+6v-6)}\\
&-\frac{(\sqrt{33}v-\sqrt{33}v^2)\epsilon^{(5)}}{6(v+1)(2v-1)(5v^2+6v-6)}\Bigg),
\end{aligned}
$$

$$
\begin{aligned}
N_{22}^{(2)} = E\Bigg(&-\frac{\sqrt{5}\hat{e}_{11}^{(0)}v^2}{2(v+1)(2v-1)(13v^2+14v-14)}\\
&-\frac{3\sqrt{5}\hat{e}_{11}^{(4)}v^2}{2(v+1)(2v-1)(13v^2+14v-14)}\\
&-\frac{\sqrt{5}\hat{e}_{22}^{(0)}v^2}{2(v+1)(2v-1)(13v^2+14v-14)}\\
&-\frac{3\sqrt{5}\hat{e}_{22}^{(4)}v^2}{2(v+1)(2v-1)(13v^2+14v-14)}\\
&-\frac{(26v^3+33v^2-28v)\hat{e}_{11}^{(2)}}{2(v+1)(2v-1)(13v^2+14v-14)}\\
&-\frac{(-26v^3+3v^2+56v-28)\hat{e}_{22}^{(2)}}{2(v+1)(2v-1)(13v^2+14v-14)}\\
&-\frac{(\sqrt{5}v-\sqrt{5}v^2)\epsilon^{(0)}}{2(v+1)(2v-1)(13v^2+14v-14)}\\
&-\frac{(26v^3+23v^2-23v)\epsilon^{(2)}}{2(v+1)(2v-1)(13v^2+14v-14)}\\
&-\frac{(3\sqrt{5}v-3\sqrt{5}v^2)\epsilon^{(4)}}{2(v+1)(2v-1)(13v^2+14v-14)}\Bigg),
\end{aligned}
$$

$$
\begin{aligned}
N_{22}^{(3)} = E\Bigg(&-\frac{\sqrt{\frac{7}{3}}\hat{e}_{11}^{(1)}v^2}{2(v+1)(2v-1)(5v^2+6v-6)}\\
&-\frac{\sqrt{77}\hat{e}_{11}^{(5)}v^2}{6(v+1)(2v-1)(5v^2+6v-6)}\\
&-\frac{\sqrt{\frac{7}{3}}\hat{e}_{22}^{(1)}v^2}{2(v+1)(2v-1)(5v^2+6v-6)}\\
&-\frac{\sqrt{77}\hat{e}_{22}^{(5)}v^2}{6(v+1)(2v-1)(5v^2+6v-6)}\\
&-\frac{(30v^3+43v^2-36v)\hat{e}_{11}^{(3)}}{6(v+1)(2v-1)(5v^2+6v-6)}\\
&-\frac{(-30v^3+v^2+72v-36)\hat{e}_{22}^{(3)}}{6(v+1)(2v-1)(5v^2+6v-6)}\\
&-\frac{(\sqrt{21}v-\sqrt{21}v^2)\epsilon^{(1)}}{6(v+1)(2v-1)(5v^2+6v-6)}\\
&-\frac{(30v^3+29v^2-29v)\epsilon^{(3)}}{6(v+1)(2v-1)(5v^2+6v-6)}\\
&-\frac{(\sqrt{77}v-\sqrt{77}v^2)\epsilon^{(5)}}{6(v+1)(2v-1)(5v^2+6v-6)}\Bigg),
\end{aligned}
$$

$$
\begin{aligned}
N_{22}^{(4)} = E\Bigg(&-\frac{3\hat{e}_{11}^{(0)}v^2}{2(v+1)(2v-1)(13v^2+14v-14)}\\
&-\frac{3\sqrt{5}\hat{e}_{11}^{(2)}v^2}{2(v+1)(2v-1)(13v^2+14v-14)}\\
&-\frac{3\hat{e}_{22}^{(0)}v^2}{2(v+1)(2v-1)(13v^2+14v-14)}\\
&-\frac{3\sqrt{5}\hat{e}_{22}^{(2)}v^2}{2(v+1)(2v-1)(13v^2+14v-14)}\\
&-\frac{(26v^3+37v^2-28v)\hat{e}_{11}^{(4)}}{2(v+1)(2v-1)(13v^2+14v-14)}\\
&-\frac{(-26v^3+7v^2+56v-28)\hat{e}_{22}^{(4)}}{2(v+1)(2v-1)(13v^2+14v-14)}\\
&-\frac{(3v-3v^2)\epsilon^{(0)}}{2(v+1)(2v-1)(13v^2+14v-14)}\\
&-\frac{(3\sqrt{5}v-3\sqrt{5}v^2)\epsilon^{(2)}}{2(v+1)(2v-1)(13v^2+14v-14)}\\
&-\frac{(26v^3+19v^2-19v)\epsilon^{(4)}}{2(v+1)(2v-1)(13v^2+14v-14)}\Bigg),
\end{aligned}
$$

$$
\begin{aligned}
N_{22}^{(5)} = E\Bigg(&-\frac{\sqrt{\frac{11}{3}}\hat{e}_{11}^{(1)}v^2}{2(v+1)(2v-1)(5v^2+6v-6)}\\
&-\frac{\sqrt{77}\hat{e}_{11}^{(3)}v^2}{6(v+1)(2v-1)(5v^2+6v-6)}\\
&-\frac{\sqrt{\frac{11}{3}}\hat{e}_{22}^{(1)}v^2}{2(v+1)(2v-1)(5v^2+6v-6)}\\
&-\frac{\sqrt{77}\hat{e}_{22}^{(3)}v^2}{6(v+1)(2v-1)(5v^2+6v-6)}\\
&-\frac{(30v^3+47v^2-36v)\hat{e}_{11}^{(5)}}{6(v+1)(2v-1)(5v^2+6v-6)}\\
&-\frac{(-30v^3+5v^2+72v-36)\hat{e}_{22}^{(5)}}{6(v+1)(2v-1)(5v^2+6v-6)}\\
&-\frac{(\sqrt{33}v-\sqrt{33}v^2)\epsilon^{(1)}}{6(v+1)(2v-1)(5v^2+6v-6)}\\
&-\frac{(\sqrt{77}v-\sqrt{77}v^2)\epsilon^{(3)}}{6(v+1)(2v-1)(5v^2+6v-6)}\\
&-\frac{(30v^3+25v^2-25v)\epsilon^{(5)}}{6(v+1)(2v-1)(5v^2+6v-6)}\Bigg),
\end{aligned}
$$

$$T_1^{(0)} = E\left(\frac{27\gamma_1^{(0)}}{28(\nu+1)} - \frac{\sqrt{5}\gamma_1^{(2)}}{28(\nu+1)} - \frac{3\gamma_1^{(4)}}{28(\nu+1)}\right),$$

$$T_1^{(1)} = E\left(\frac{11\gamma_1^{(1)}}{12(\nu+1)} - \frac{\sqrt{\frac{7}{3}}\gamma_1^{(3)}}{12(\nu+1)} - \frac{\sqrt{\frac{11}{3}}\gamma_1^{(5)}}{12(\nu+1)}\right),$$

$$T_1^{(2)} = E\left(-\frac{\sqrt{5}\gamma_1^{(0)}}{28(\nu+1)} + \frac{23\gamma_1^{(2)}}{28(\nu+1)} - \frac{3\sqrt{5}\gamma_1^{(4)}}{28(\nu+1)}\right),$$

$$T_1^{(3)} = E\left(-\frac{\sqrt{\frac{7}{3}}\gamma_1^{(1)}}{12(\nu+1)} + \frac{29\gamma_1^{(3)}}{36(\nu+1)} - \frac{\sqrt{77}\gamma_1^{(5)}}{36(\nu+1)}\right),$$

$$T_1^{(4)} = E\left(-\frac{3\gamma_1^{(0)}}{28(\nu+1)} - \frac{3\sqrt{5}\gamma_1^{(2)}}{28(\nu+1)} + \frac{19\gamma_1^{(4)}}{28(\nu+1)}\right),$$

$$T_1^{(5)} = E\left(-\frac{\sqrt{\frac{11}{3}}\gamma_1^{(1)}}{12(\nu+1)} - \frac{\sqrt{77}\gamma_1^{(3)}}{36(\nu+1)} + \frac{25\gamma_1^{(5)}}{36(\nu+1)}\right),$$

$$T_2^{(0)} = E\left(\frac{27\gamma_2^{(0)}}{28(\nu+1)} - \frac{\sqrt{5}\gamma_2^{(2)}}{28(\nu+1)} - \frac{3\gamma_2^{(4)}}{28(\nu+1)}\right),$$

$$T_2^{(1)} = E\left(\frac{11\gamma_2^{(1)}}{12(\nu+1)} - \frac{\sqrt{\frac{7}{3}}\gamma_2^{(3)}}{12(\nu+1)} - \frac{\sqrt{\frac{11}{3}}\gamma_2^{(5)}}{12(\nu+1)}\right),$$

$$T_2^{(2)} = E\left(-\frac{\sqrt{5}\gamma_2^{(0)}}{28(\nu+1)} + \frac{23\gamma_2^{(2)}}{28(\nu+1)} - \frac{3\sqrt{5}\gamma_2^{(4)}}{28(\nu+1)}\right),$$

$$T_2^{(3)} = E\left(-\frac{\sqrt{\frac{7}{3}}\gamma_2^{(1)}}{12(\nu+1)} + \frac{29\gamma_2^{(3)}}{36(\nu+1)} - \frac{\sqrt{77}\gamma_2^{(5)}}{36(\nu+1)}\right),$$

$$T_2^{(4)} = E\left(-\frac{3\gamma_2^{(0)}}{28(\nu+1)} - \frac{3\sqrt{5}\gamma_2^{(2)}}{28(\nu+1)} + \frac{19\gamma_2^{(4)}}{28(\nu+1)}\right),$$

$$T_2^{(5)} = E\left(-\frac{\sqrt{\frac{11}{3}}\gamma_2^{(1)}}{12(\nu+1)} - \frac{\sqrt{77}\gamma_2^{(3)}}{36(\nu+1)} + \frac{25\gamma_2^{(5)}}{36(\nu+1)}\right),$$

$$\begin{aligned}\Sigma^{(0)} = E\Bigg(&-\frac{(26\nu^3+27\nu^2-27\nu)\hat{e}_{11}^{(0)}}{2(\nu+1)(2\nu-1)(13\nu^2+14\nu-14)}\\ &-\frac{(\sqrt{5}\nu-\sqrt{5}\nu^2)\hat{e}_{11}^{(2)}}{2(\nu+1)(2\nu-1)(13\nu^2+14\nu-14)}\\ &-\frac{(3\nu-3\nu^2)\hat{e}_{11}^{(4)}}{2(\nu+1)(2\nu-1)(13\nu^2+14\nu-14)}\\ &-\frac{(26\nu^3+27\nu^2-27\nu)\hat{e}_{22}^{(0)}}{2(\nu+1)(2\nu-1)(13\nu^2+14\nu-14)}\\ &-\frac{(\sqrt{5}\nu-\sqrt{5}\nu^2)\hat{e}_{22}^{(2)}}{2(\nu+1)(2\nu-1)(13\nu^2+14\nu-14)}\\ &-\frac{(3\nu-3\nu^2)\hat{e}_{22}^{(4)}}{2(\nu+1)(2\nu-1)(13\nu^2+14\nu-14)}\\ &-\frac{(-26\nu^3-\nu^2+54\nu-27)\epsilon^{(0)}}{2(\nu+1)(2\nu-1)(13\nu^2+14\nu-14)}\\ &-\frac{(\sqrt{5}\nu^2-2\sqrt{5}\nu+\sqrt{5})\epsilon^{(2)}}{2(\nu+1)(2\nu-1)(13\nu^2+14\nu-14)}\\ &-\frac{(3\nu^2-6\nu+3)\epsilon^{(4)}}{2(\nu+1)(2\nu-1)(13\nu^2+14\nu-14)}\Bigg),\end{aligned}$$

$$\begin{aligned}\Sigma^{(1)} = E\Bigg(&-\frac{(30\nu^3+33\nu^2-33\nu)\hat{e}_{11}^{(1)}}{6(2\nu^2+\nu-1)(5\nu^2+6\nu-6)}\\ &-\frac{(\sqrt{21}\nu-\sqrt{21}\nu^2)\hat{e}_{11}^{(3)}}{6(2\nu^2+\nu-1)(5\nu^2+6\nu-6)}\\ &-\frac{(\sqrt{33}\nu-\sqrt{33}\nu^2)\hat{e}_{11}^{(5)}}{6(2\nu^2+\nu-1)(5\nu^2+6\nu-6)}\\ &-\frac{(30\nu^3+33\nu^2-33\nu)\hat{e}_{22}^{(1)}}{6(2\nu^2+\nu-1)(5\nu^2+6\nu-6)}\\ &-\frac{(\sqrt{21}\nu-\sqrt{21}\nu^2)\hat{e}_{22}^{(3)}}{6(2\nu^2+\nu-1)(5\nu^2+6\nu-6)}\\ &-\frac{(\sqrt{33}\nu-\sqrt{33}\nu^2)\hat{e}_{22}^{(5)}}{6(2\nu^2+\nu-1)(5\nu^2+6\nu-6)}\\ &-\frac{(-30\nu^3-3\nu^2+66\nu-33)\epsilon^{(1)}}{6(2\nu^2+\nu-1)(5\nu^2+6\nu-6)}\\ &-\frac{(\sqrt{21}\nu^2-2\sqrt{21}\nu+\sqrt{21})\epsilon^{(3)}}{6(2\nu^2+\nu-1)(5\nu^2+6\nu-6)}\\ &-\frac{(\sqrt{33}\nu^2-2\sqrt{33}\nu+\sqrt{33})\epsilon^{(5)}}{6(2\nu^2+\nu-1)(5\nu^2+6\nu-6)}\Bigg),\end{aligned}$$

$$\begin{aligned}\Sigma^{(2)} = E\Bigg(&-\frac{(\sqrt{5}\nu-\sqrt{5}\nu^2)\hat{e}_{11}^{(0)}}{2(\nu+1)(2\nu-1)(13\nu^2+14\nu-14)}\\ &-\frac{(26\nu^3+23\nu^2-23\nu)\hat{e}_{11}^{(2)}}{2(\nu+1)(2\nu-1)(13\nu^2+14\nu-14)}\\ &-\frac{(3\sqrt{5}\nu-3\sqrt{5}\nu^2)\hat{e}_{11}^{(4)}}{2(\nu+1)(2\nu-1)(13\nu^2+14\nu-14)}\\ &-\frac{(\sqrt{5}\nu-\sqrt{5}\nu^2)\hat{e}_{22}^{(0)}}{2(\nu+1)(2\nu-1)(13\nu^2+14\nu-14)}\\ &-\frac{(26\nu^3+23\nu^2-23\nu)\hat{e}_{22}^{(2)}}{2(\nu+1)(2\nu-1)(13\nu^2+14\nu-14)}\\ &-\frac{(3\sqrt{5}\nu-3\sqrt{5}\nu^2)\hat{e}_{22}^{(4)}}{2(\nu+1)(2\nu-1)(13\nu^2+14\nu-14)}\\ &-\frac{(\sqrt{5}\nu^2-2\sqrt{5}\nu+\sqrt{5})\epsilon^{(0)}}{2(\nu+1)(2\nu-1)(13\nu^2+14\nu-14)}\\ &-\frac{(-26\nu^3+3\nu^2+46\nu-23)\epsilon^{(2)}}{2(\nu+1)(2\nu-1)(13\nu^2+14\nu-14)}\\ &-\frac{(3\sqrt{5}\nu^2-6\sqrt{5}\nu+3\sqrt{5})\epsilon^{(4)}}{2(\nu+1)(2\nu-1)(13\nu^2+14\nu-14)}\Bigg),\end{aligned}$$

$$\Sigma^{(3)} = E\Bigg(-\frac{(\sqrt{21}v-\sqrt{21}v^2)\hat{e}_{11}^{(1)}}{6(2v^2+v-1)(5v^2+6v-6)} - \frac{(30v^3+29v^2-29v)\hat{e}_{11}^{(3)}}{6(2v^2+v-1)(5v^2+6v-6)} - \frac{(\sqrt{77}v-\sqrt{77}v^2)\hat{e}_{11}^{(5)}}{6(2v^2+v-1)(5v^2+6v-6)} - \frac{(\sqrt{21}v-\sqrt{21}v^2)\hat{e}_{22}^{(1)}}{6(2v^2+v-1)(5v^2+6v-6)} - \frac{(30v^3+29v^2-29v)\hat{e}_{22}^{(3)}}{6(2v^2+v-1)(5v^2+6v-6)} - \frac{(\sqrt{77}v-\sqrt{77}v^2)\hat{e}_{22}^{(5)}}{6(2v^2+v-1)(5v^2+6v-6)} - \frac{(\sqrt{21}v^2-2\sqrt{21}v+\sqrt{21})\epsilon^{(1)}}{6(2v^2+v-1)(5v^2+6v-6)} - \frac{(-30v^3+v^2+58v-29)\epsilon^{(3)}}{6(2v^2+v-1)(5v^2+6v-6)} - \frac{(\sqrt{77}v^2-2\sqrt{77}v+\sqrt{77})\epsilon^{(5)}}{6(2v^2+v-1)(5v^2+6v-6)}\Bigg),$$

$$\Sigma^{(4)} = E\Bigg(-\frac{(3v-3v^2)\hat{e}_{11}^{(0)}}{2(v+1)(2v-1)(13v^2+14v-14)} - \frac{(3\sqrt{5}v-3\sqrt{5}v^2)\hat{e}_{11}^{(2)}}{2(v+1)(2v-1)(13v^2+14v-14)} - \frac{(26v^3+19v^2-19v)\hat{e}_{11}^{(4)}}{2(v+1)(2v-1)(13v^2+14v-14)} - \frac{(3v-3v^2)\hat{e}_{22}^{(0)}}{2(v+1)(2v-1)(13v^2+14v-14)} - \frac{(3\sqrt{5}v-3\sqrt{5}v^2)\hat{e}_{22}^{(2)}}{2(v+1)(2v-1)(13v^2+14v-14)} - \frac{(26v^3+19v^2-19v)\hat{e}_{22}^{(4)}}{2(v+1)(2v-1)(13v^2+14v-14)} \times \frac{(3v^2-6v+3)\epsilon^{(0)}}{2(v+1)(2v-1)(13v^2+14v-14)} - \frac{(3\sqrt{5}v^2-6\sqrt{5}v+3\sqrt{5})\epsilon^{(2)}}{2(v+1)(2v-1)(13v^2+14v-14)} - \frac{(-26v^3+7v^2+38v-19)\epsilon^{(4)}}{2(v+1)(2v-1)(13v^2+14v-14)}\Bigg),$$

$$\Sigma^{(5)} = E\Bigg(-\frac{(\sqrt{33}v-\sqrt{33}v^2)\hat{e}^{(1)}}{6(2v^2+v-1)(5v^2+6v-6)} - \frac{(\sqrt{77}v-\sqrt{77}v^2)\hat{e}_{11}^{(3)}}{6(2v^2+v-1)(5v^2+6v-6)} - \frac{(30v^3+25v^2-25v)\hat{e}_{11}^{(5)}}{6(2v^2+v-1)(5v^2+6v-6)} - \frac{(\sqrt{33}v-\sqrt{33}v^2)\hat{e}_{22}^{(1)}}{6(2v^2+v-1)(5v^2+6v-6)} - \frac{(\sqrt{77}v-\sqrt{77}v^2)\hat{e}_{22}^{(3)}}{6(2v^2+v-1)(5v^2+6v-6)} - \frac{(30v^3+25v^2-25v)\hat{e}_{22}^{(5)}}{6(2v^2+v-1)(5v^2+6v-6)} - \frac{(\sqrt{33}v^2-2\sqrt{33}v+\sqrt{33})\epsilon^{(1)}}{6(2v^2+v-1)(5v^2+6v-6)} - \frac{(\sqrt{77}v^2-2\sqrt{77}v+\sqrt{77})\epsilon^{(3)}}{6(2v^2+v-1)(5v^2+6v-6)} - \frac{(-30v^3+5v^2+50v-25)\epsilon^{(5)}}{6(2v^2+v-1)(5v^2+6v-6)}\Bigg).$$

References

[1] Reddy JN. A simple higher-order theory for laminated composite plates. J Appl Mech 1984;51:745–52.

[2] Hanna NF, Leissa AW. A higher order shear deformation theory for the vibration of thick plates. J Sound Vibrat 1994;170:545–55.

[3] Mindlin RC, Medick MA. Extensional vibrations of elastic plates. J Appl Mech 1959;26:145–51.

[4] Soldatos KP, Watson P. Accurate stress analysis of laminated plates combining two-dimensional theory with the exact three-dimensional solution for simply supported edges. Math Mech Solids 1997;2:459–89.

[5] Babu CS, Kant T. Refined higher-order finite element models for thermal buckling of laminated composites and sandwich plates. J Therm Stress 2000;23:111–30.

[6] Chao CC, Chung TP, Sheu CC, Tseng JH. A consistent higher-order theory of laminated plates with nonlinear impact modal analysis. J Vibrat Acoust 1994;116:371–8.

[7] Lee PC-Y, Yu JD. Governing equations of piezoelectric plates with graded properties across the thickness. IEEE Trans Ultrason, Ferroelect Frequency Contr 1998;45:236–50.

[8] Batra RC, Vidoli S. Higher order piezoelectric plate theory derived from a three-dimensional variational principle. AIAA J 2002;40:91–104.

[9] Messina A. Two generalized higher order theories in free vibration studies of multilayered plates. J Sound Vibrat 2001;242:125–50.

[10] Carrera E. A study of transverse normal stress effect on vibration of multilayered plates and shells. J Sound Vibrat 1999;225:803–29.

[11] Di Carlo A, Podio-Guidugli P, Williams WO. Shells with thickness distension. Int J Solids Struct 2001;38:1201–25.

[12] Cosserat E, Cosserat F. Sur la statique de la ligne deformable. CR Hebdomad Sea Acad Sci 1907;145:1409–12.

[13] Batra RC, Vidoli S, Vestroni F. Plane waves and modal analysis in higher-order shear and normal deformable plate theories. J Sound Vibrat 2002;257:63–88.

[14] Srinivas S, Joga Rao CV, Rao AK. An exact analysis for vibration of simply supported homogeneous and laminate thick rectangular plates. J Sound Vibrat 1970;12:187–99.

[15] Batra RC, Aimmanee S. Missing frequencies in previous exact solutions of free vibrations of simply supported rectangular plates. J Sound Vibrat 2003;265:887–96.
[16] Soldatos KP, Hadjigergiou VP. Three-dimensional solution of the free vibration problem of homogeneous isotropic cylindrical shells and panels. J Sound Vibrat 1990;137:369–84.
[17] Liew KM, Hung KC, Lim MK. Three-dimensional vibration of rectangular plates: effects of thickness and edge constraints. J Sound Vibrat 1995;182:709–27.
[18] Qian LF, Batra RC, Chen LM. Free and forced vibrations of thick rectangular plates by using higher-order shear and normal deformable plate theory and meshless local Petrov–Galerkin method. Comput Model Eng Sci 2003;4:519–34.
[19] Vel SS, Batra RC. Cylindrical bending of laminated plates with distributed and segmented piezoelectric actuators/sensors. AIAA J 2000;38:857–67.
[20] Liew KM, Teo TM. Three-dimensional vibration analysis of rectangular plates based on differential quadrature method. J Sound Vibrat 1999;220:577–99.
[21] Batra RC, Qian LF, Chen LM. Natural frequencies of thick square plates made of orthotropic, trigonal, monoclinic, hexagonal and triclinic materials. J Sound Vibrat 2004;27:1074–86.
[22] Vel SS, Batra RC. Three dimensional exact solution for the vibration of functionally graded rectangular plates. J Sound Vibrat 2004;272:703–30.
[23] Yang JS, Batra RC. Mixed variational principles in nonlinear piezoelectricity. Int J Nonlinear Mech 1995;30:719–26.
[24] Batra RC, Liang XQ. The vibration of a rectangular laminated elastic plate with embedded piezoelectric sensors and actuators. Comput Struct 1997;63:203–16.
[25] Qian LF, Batra RC, Chen LM. Static and dynamic deformations of thick functionally graded elastic plate by using higher-order shear and normal deformable plate theory and meshless local Petrov–Galerkin method. Composites: Part B 2004;35:685–97.
[26] Qian LF, Batra RC. Design of bidirectional functionally graded plate for optimal natural frequencies. J Sound Vibrat 2005;280:415–24.
[27] Qian LF, Batra RC. Transient thermoelastic deformations of a thick functionally graded plate. J Thermal Stresses 2004;27:705–40.
[28] Qian LF, Batra RC. Three-dimensional transient heat conduction in a functionally graded thick plate with a higher-order plate theory and a meshless local Petrov–Galerkin method. Computational Mechanics 2005;35:214–26.